國立臺灣大學醫學院暨工學院醫學工程學系

博士論文

Department of Biomedical Engineering
College of Medicine and College of Engineering
National Taiwan University
Doctoral Dissertation

步態機械能量流分析與臨床應用

Mechanical Energy Flow Analysis and Clinical Applications on Human Walking

陳鴻彬

Hung-Bin Chen

指導教授：黃義侑 博士 、章良渭 博士

Advisor: Yi-You Huang, Ph.D., Liang-Wey Chang, Ph.D.

中華民國 108 年 7 月
July, 2019

doi:10.6342/NTU201901683

中文摘要

背景：

機械能量流為整合運動學與力動學資料之數學量，可將片段之肢段運動與關節角度、力矩、功率等資訊整合成完整且系統性的構圖，清晰地顯現致使動作產生的能量來龍去脈。如何表達與應用其深厚與豐富的內涵成為本研究的重點目標。本研究的目的是建立能量流模型，並應用此模型深入探討正常人步態之能量流動特徵與動作策略。

方法：

本研究使用三維動作分析系統收集正常年輕人與正常老年人的步態資料，經由整合下肢各肢段與關節之能量流數據，建構出正常年輕人於 push-off 時期之能量流動路徑圖，並使用因素分析，萃取並比較正常年輕人與正常老年人於不同步行速度下之擺盪期(swing phase)能量流動特徵。

結果：

收集八名正常年輕人資料的研究結果顯示在 push-off 時期，踝關節產生之能量絕大多數是用以提昇同側肢段之動能，而傳遞至骨盆的能量僅是踝關節產生最大能量值之 10%。收集十名正常年輕人與十名正常老年人資料的因素分析結果顯示，正常年輕人於自選步行速度與快速步行之情況下，皆呈現相似地擺盪期能量流動特徵。而正常老年人於快速步行之情況下，其擺盪期能量流動特徵與自選步行速度下之呈現特徵相反。

結論：

本研究已開發一個能量流模型，建立關節能與肢段能之橋段，其中關鍵之能量流參數可對應到現今習用之動作分析參數如關節功率與肢段動位能變化率等。透過觀察與分析模型中機械能之流動特徵，可直覺式地推論動作策略的能量調節機制，提供臨床研究人員從整體探討動作策略與能量使用效率之有利工具。本研究亦嘗試提供另一種能量流模型之應用方法，從高維度之能量流資料中，使用因素分析來比較不同族群間能量流動模式之差異。

doi:10.6342/NTU201901683

關鍵詞: 步態、能量流、生物力學、老化、因素分析

doi:10.6342/NTU201901683

Abstract

Background:

Mechanical energy flow of human movement is an integrated presentation of kinematics and kinetics, which provides a systematic picture and potentially could be a powerful tool for clinicians and researchers to look into the movement strategies and energy efficiency of human movement. The purpose of this research is to develop an energy flow model with a perspective on bridging joint and segmental energetics. The energy flow model is utilized to investigate walking strategy adopted by the healthy young adults and the elders in order to demonstrate clinical applications of the developed energy flow model.

Method:

Healthy young adults and healthy elders were be recruited in this research. Gait data of all participants were captured by three-dimensional motion capture system. Energetic data of the pelvis and lower limb were used to construct an energy flow diagram at the instant of peak ankle power generation during push-off in young adults. The factor analysis was then applied to extract the high-dimensional energy flow characteristics of the swing leg in young adults and the elders.

doi:10.6342/NTU201901683

Results:

Results of 8 healthy young adults suggest that the ankle mainly contributes to increase the kinetic energy of the ipsilateral leg in preparation for swing during push-off. The magnitude of the power flowing to the pelvis, which could be used for forward propulsion, was only 10% of that generated by the ankle. The results of factor analysis of 10 healthy young adults and 10 healthy elders showed that the young adults have similar energy flow characteristics of the swing leg for both fast and self-selected walking speeds, while the elderly showed an opposite energy flow pattern especially at the fast walking speed. The hip power and the knee power were also found to mainly correspond to the swing acceleration and deceleration, respectively.

Conclusions:

A new symbolic convention of energy flow diagram was developed to manifest where the generated ankle power is transmitted to in order to ease of interpreting the function of the ankle. By comparing the energy flow characteristics of the elders with young adults, this research demonstrated a valuable tool to explore the change of the gait characteristics in the elderly and could help to facilitate the understanding of the neuromuscular adaptation due to aging. The proposed energy flow analysis is also a

doi:10.6342/NTU201901683

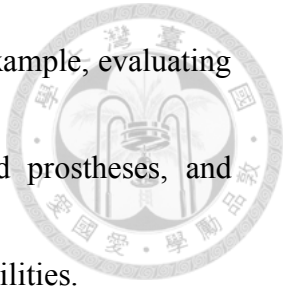

useful analytic tool with applications across many disciplines, for example, evaluating the energy performance of elite athletes, designing the powered prostheses, and revealing the compensatory movement strategy of people with disabilities.

Keywords: Ankle power, Push-off, Biomechanics, Energy flow, Gait, Aging, Swing

doi:10.6342/NTU201901683

Contents

doi:10.6342/NTU201901683

doi:10.6342/NTU201901683

doi:10.6342/NTU201901683

List of Figures

doi:10.6342/NTU201901683

doi:10.6342/NTU201901683

List of Tables

doi:10.6342/NTU201901683

Chapter 1

Introduction

1.1 Research Motivations

Human movement strategy is a critical topic in many disciplines including rehabilitation, orthopedics, and sports medicine. Many studies have attempted to interpret the movement strategy via the kinematic, kinetic, and/or electromyographic data but only a few are from a systematic perspective. Energetic analysis requires integrating kinematic and kinetic data, in which results also correlate to the electromyographic data well. Hence, a model that can link the energetic data of multiple joints and segments together would be a valuable tool to systematically explore the human movement strategy.

1.2 Literature Review

1.2.1 Development of the energy flow model

Comprehensive walking energetics analysis should consider both segmental and joint energetics. In 1978, Winter and Robertson proposed an energy flow model to analyze the gait energetics in a systematic view of segmental and joint energetics [1]. Figure 1-1 showed an example of the energy flow between joints and segments at push-

doi:10.6342/NTU201901683

off phase represented in the original model proposed by Winter [1]. All forms of mechanical energies of joints and segments including joint linear power, joint angular power, segmental potential energy change, segmental linear kinetic energy change, and segmental angular kinetic energy change were linked within the model. The benefit of the energy flow analysis is the unique capability to identify the cause of a specific flowing pattern between joints and segments, i.e. movement strategy.

However, for more than three decades, the model was not used except a few research utilizing the model to investigate the power distribution and mechanical energy of upper-extremities for studies in wheelchair design parameters and propulsion [2-4]. Possible reasons are 1) No attempt was made in Winter's model to draw conclusions of human movement strategy and therefore clinical meaning of energy distribution could not be easily understood, 2) The model was not intuitive to interpret the movement strategy from observing joint power utilization because the role of the joint power was not explicitly revealed in model presentation, and 3) It's difficult for clinicians to implement the model because the energy flow analysis is not readily available from the built-in software of motion analysis systems.

doi:10.6342/NTU201901683

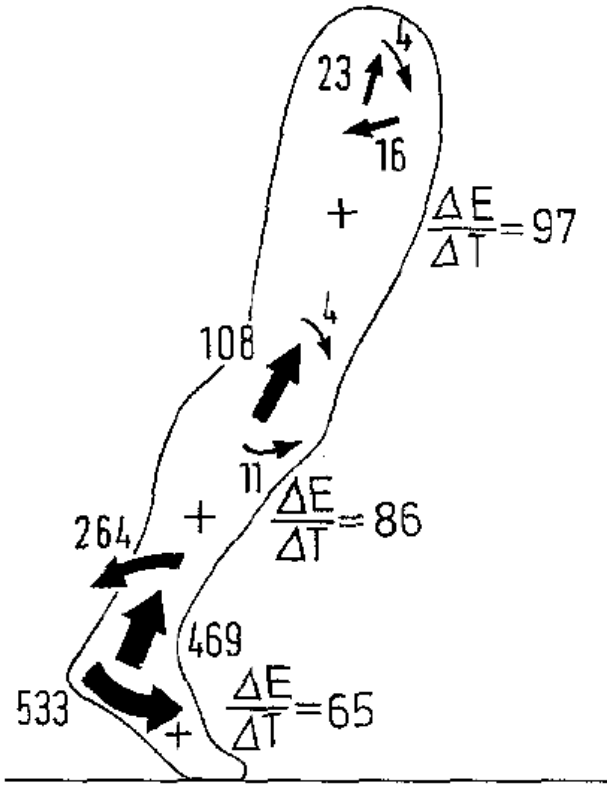

Figure 1-1 The energy flows between joints and segments at push-off presented in the original energy flow model proposed by Winter (cited from [1]). The straight arrow represents linear joint power and the curved arrow represents angular joint power. Segmental power is presented as $\frac{\Delta E}{\Delta T}$.

1.2.2 Movement strategy of walking during ankle push-off

It has been widely accepted that the ankle generates most of the mechanical power during push-off in human walking. The ankle can generate power about 2.13 W/kg-m in young adults and can produce work about 0.296 J/kg in a single step during push-

doi:10.6342/NTU201901683

off [5, 6]. Since the ankle generates the most work during push-off, previous studies have speculated that ankle power would be one of the key sources of mechanical power for forward propulsion [7, 8]. However, simple walking models have demonstrated that walking without ankle power is possible on a sloped surface [9, 10]. The robotic Delft biped also demonstrates this concept by using powered hip joints and passive ankles to achieve a mechanical cost of transport slightly higher than that of humans [11, 12]. These findings may imply that the walking task can still be completed by increasing the power generated by other lower limb segments other than the ankle while it was recognized that the ankle joint generates a large power for body propulsion during the late stance phase.

Studies on the role of ankle power during push-off in human walking have not reached a consensus. Some studies suggest that ankle power does not propel the trunk forward during push-off, but rather actuates the foot to simulate a rocker which allows the trunk smoothly "roll over" [13-15]. Other studies propose that the ankle primarily accelerates the leg just prior to swing phase [16-18]. A bipedal robot and a corresponding computer simulation show how the ankle can assist ipsilateral leg swing during push-off [19]; however, simulations of leg muscle action suggest that the ankle

doi:10.6342/NTU201901683

plays a major role in trunk propulsion during push-off [20, 21]. Recent research has demonstrated the effect of the ankle during push-off on reducing metabolic energy expenditure, and proposes that the ankle assists leg swing rather than decreases limb collision during push-off [22]. These arguments make the role of the ankle during push-off controversial since no method has empirically demonstrated the movement strategy during ankle push-off in human walking.

1.2.3 Movement strategy of walking in the elders

Blanke et al. concluded that the healthy young and the healthy elderly men have similar gait characteristics on kinematics in terms of step and stride length, velocity, ankle range of motion, vertical and horizontal excursions of the center of gravity, and pelvic obliquity [23]. Chung et al. also reported similar results of age effect on joint motions but the EMG of the rectus femoris was significantly more active in the older group [24]. Boyer et al. in their recent research showed the older adults maintain the walking speed by increasing cadence while reducing stride-length. They present with slightly smaller ankle dorsiflexion moments but greater hip extensor moments than the young adults [25]. Regarding the walking energetics, DeVita et al. showed that age causes a redistribution on joint moments and powers and they considered this

doi:10.6342/NTU201901683

redistribution as an alteration in the motor pattern used to perform the task [26]. Graf et al. also reported that the lower-performing elderly generated significantly lower ankle plantarflexor power during late stance but significantly higher hip extensor power during early stance than the healthy elderly [27]. Change of gait performance could be driven by the altered neuromuscular control since the physical degenerations need to be compensated by adjusting the kinematic and kinetic coordination of the body. Previous studies had reported that the healthy elderly showed reduced ankle plantarflexion angle/moment/power, reduced knee flexion angle, reduced knee extension moment/power, reduced hip extension angle, and increased hip flexion/extension moment/power [27-30]. These evidences suggested that aging could lead to neuromuscular adaption of the lower extremity that occurs in multiple joints rather than a single one.

During the swing phase of the gait cycle, the elderly has been reported to exhibit greater toe clearance variability than the young adults [31, 32], while the variability should be minimized to avoid the occurrence of toe-ground contact events. Tripping occurred during the swing phase of walking had been reported to be responsible for 53% of falls in elderly [33]. Previous studies also reported that, while making a rapid

doi:10.6342/NTU201901683

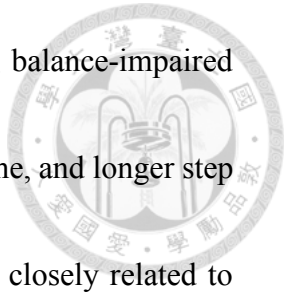

voluntary forward step for the advancement of the lower extremity, balance-impaired older adults demonstrate smaller step length, slower step reaction time, and longer step time than balance-unimpaired older adults, and these measures are closely related to fall risks [34-36]. These findings highlight the importance to identify the age-related changes of the movement strategy during the swing phase that may predispose the elderly to slipping or tripping.

Energy flow analysis had been utilized to investigate the mechanical powers across multiple segments and joints [1, 37]. A previous study found an energy flow disruption prior to push-off in elderly that is an altered hip mechanics to compensate the ankle plantarflexor weakness during a fast walking [38]. Another study also found that the elderly with orthopedic problems spend more hip mechanical energy to compensate for the weak ankle plantarflexor [35]. However, previous studies mostly focused only on specific gait events, e.g. at the instance of the foot push-off, which may not be able to identify the comprehensive neuromuscular adaptation of a gait cycle. It can be very challenging to analyze the energy flow characteristics of different gait phases due to the high-dimensionality, temporal-dependence, and high variability of the dataset. To our knowledge, there is no systematic approach to characterize the energy

doi:10.6342/NTU201901683

flow pattern during the entire phases, either the stance phase or the swing phase, of the gait.

1.3 Research Objectives

The main purpose of this research is to propose a new convention of the energy flow model for intuitively interpreting the movement strategy according to the observed energy flow characteristics. The energy flow characteristics refer to the flow pattern and energy distribution among joints and segments. Research procedure is shown in Figure 1-2. The proposed model utilizes a new perspective for bridging the joint and segmental energetics in order to make each term of energy flow within the new model easy to comprehend. Consequently, interpreting movement strategy will become very intuitive. Another feature of the new model will be easy to implement. The advantages of the new model will be demonstrated via analyzing the gait trials of healthy young adults and elders walking at different speeds. The proposed energy flow model will have a significant impact on improving the design of assistive devices for locomotion and suggesting clinical interventions on rehabilitation, orthopedics, and sports medicine.

doi:10.6342/NTU201901683

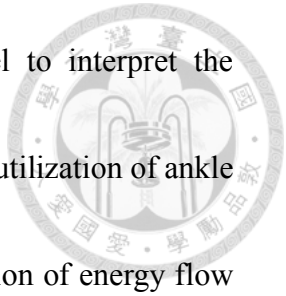

In order to demonstrate how to utilize the proposed model to interpret the movement strategy, the first clinical application is to investigate the utilization of ankle power generated during push-off by using a new symbolic convention of energy flow diagram. We used energy flow analysis techniques developed by Winter and Robertson [1]. In addition to improving the clarity of visual presentation of the energy flow analysis, we proposed a new symbolic convention to provide a self-interpreting energy flow diagram. This diagram, with the new convention, would manifest the flow of mechanical energy and how joint power is utilized in the leg by combining the joint and segmental energetics. It was hypothesized for the experiment that the ankle power generated during push-off would primarily increase the energy of ipsilateral limb segments rather than the pelvis. To test this hypothesis, an energy flow diagram was constructed from the data collected at the instant of peak ankle power generation, and the ankle power utilization was then analyzed.

The second clinical application is to identify the important factors that control the swing leg and to compare the energy flow characteristics of the swing phase during level walking in young adults and the elderly. Factor analysis would be utilized to extract the characteristics of the energy flows from a high-dimensional dataset. Our

doi:10.6342/NTU201901683

research hypothesis was that the elderly presents distinct energy flow characteristics that unveil the altered coordination among the segments of the lower extremity during the swing phase. Our work would help to facilitate the understanding of the neuromuscular adaptation due to aging, which can potentially contribute to the fall prevention, orthopedic treatments and rehabilitation interventions for elderly.

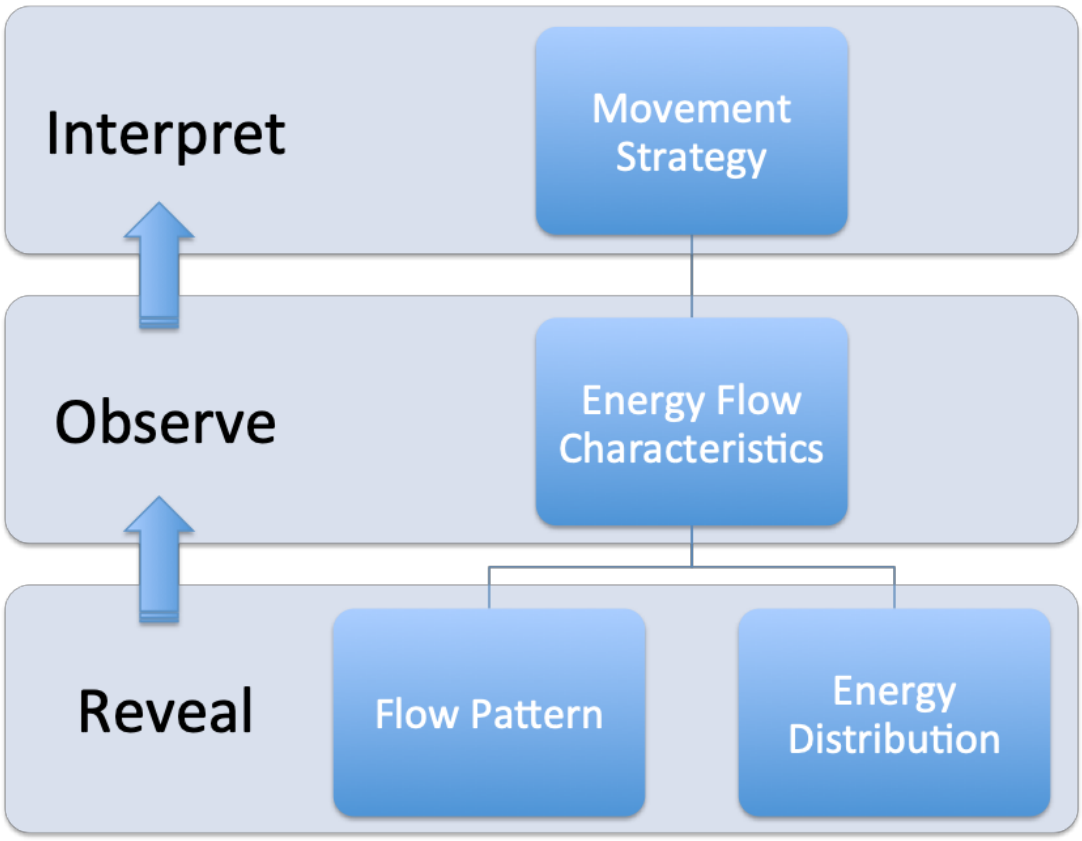

Figure 1-2 Research procedure of this project. The movement strategy will be interpreted by observing energy flow characteristics in terms of flow pattern and energy distribution

doi:10.6342/NTU201901683

Chapter 2

Materials and Methods

2.1 Subjects

Healthy young adults and healthy elders were recruited in this research. Exclusion criteria included the inability to follow instructions, cardiopulmonary dysfunctions, joint replacements in the lower extremities, arthritis, diabetes, vestibular deficits, or any type of neuromusculoskeletal problems that could interfere with the gait pattern. All the participants were right foot dominant, defined as the preferred leg for kicking a ball. The experimental protocol was approved by and performed in accordance with the relevant guidelines and regulations of the Research Ethics Committee of National Taiwan University Hospital (No. 201112121RIC). All subjects had provided their signed informed consents before participating in the study. The blank informed consent was shown in Appendix I.

2.2 Instrumentation

Two optoelectric position sensors (Optotrak Certus, Northern Digital Inc., Waterloo, Canada) were used to collect kinematic data during gait (Figure 2-1.a).

doi:10.6342/NTU201901683

Rigid bodies which contain three infrared-emitting diodes (IRED) in each set are respectively attached on lower limb segments (Figure 2-1.b) and thus the segment-fixed coordinate systems can then be established and tracked. By finishing the procedure of digitizing segmental landmarks while the presence of the rigid bodies at static standing posture (Figure 2-1.d), spatial coordinates of segmental landmarks can then be tracked. Kinetic data were collected with two force platforms (Accugait, Advanced Mechanical Technology Inc., Massachusetts, USA) (Figure 2-1.c). Both kinematic and kinetic data were collected synchronously at the sampling rate of 50 Hz via a program developed in LabVIEW 14.0 (National Instruments, Texas, USA) (Figure 2-2). An overview of the instrumentation setup in this research was shown in Figure 2-3.

doi:10.6342/NTU201901683

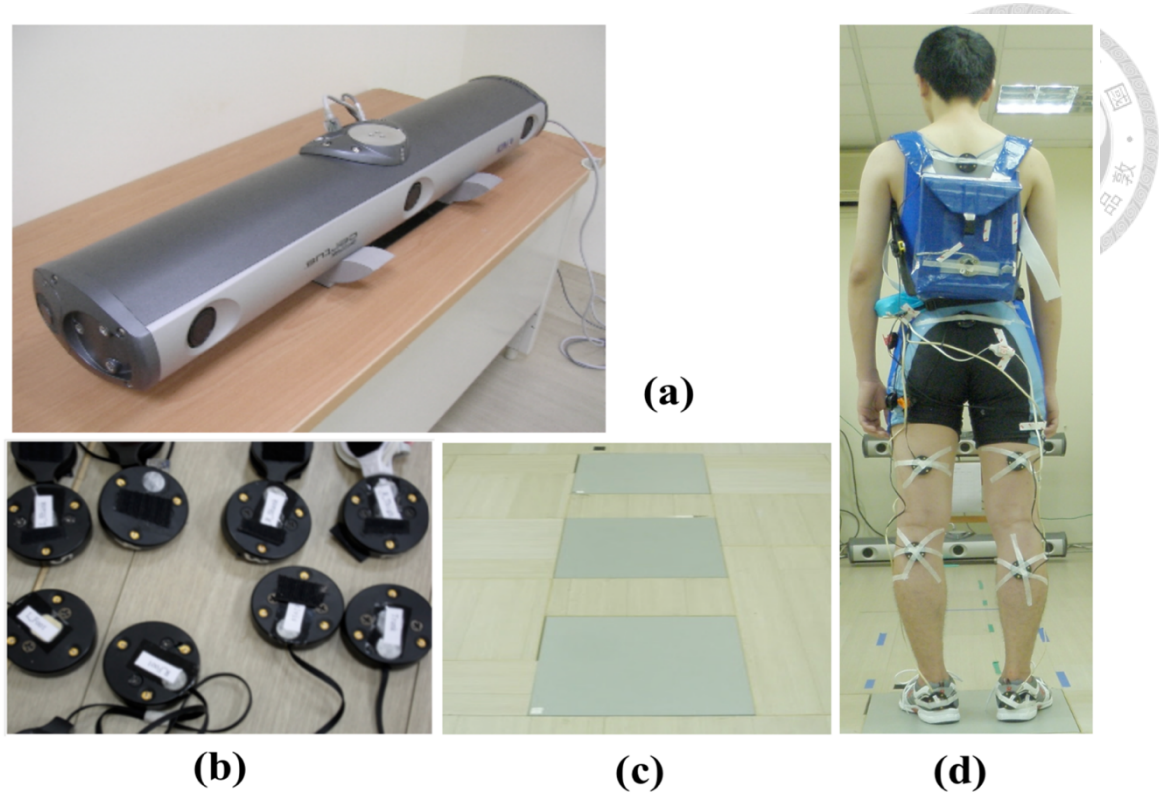

Figure 2-1 (a) Optoelectric position sensor to track marker trajectory ; (b) rigid bodies that contain three active markers in each set ; (c) force plates that are embedded in the floor ; and (d) Apply rigid bodies on the subject.

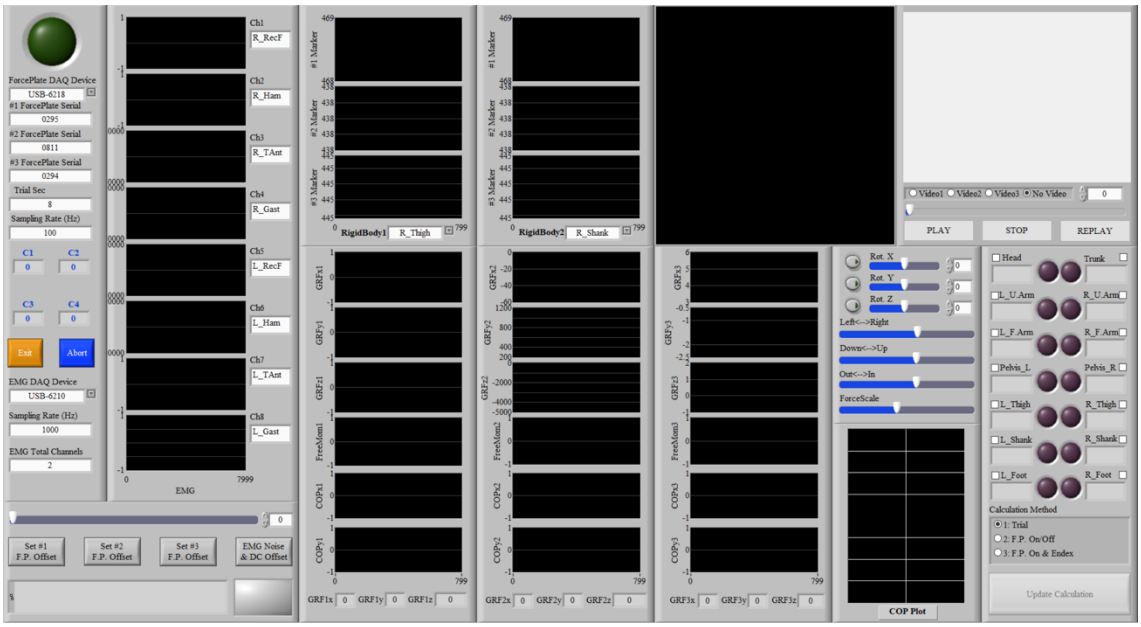

Figure 2-2 LabVIEW program developed to collect gait trials for energy flow analysis

doi:10.6342/NTU201901683

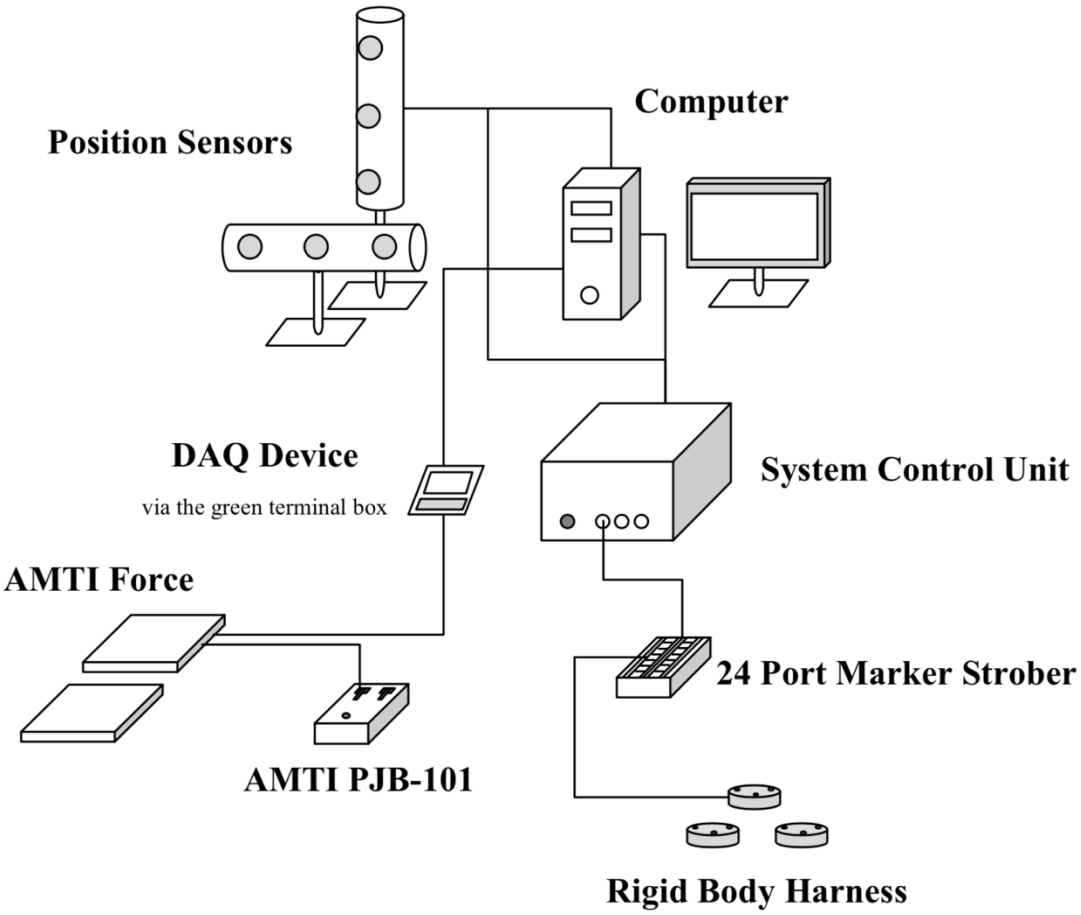

Figure 2-3 An overview of the instrumentation setup in this research

doi:10.6342/NTU201901683

2.3 Experimental Protocol

All subjects walked with shoes along a 10-meter walkway at the self-selected speed and the fast speed respectively. The instruction for the fast speed was to ask the subject simulating a functional task, i.e. crossing a street as fast as possible when the green light is about to turn red in 10 seconds. Each subject was allowed to practice and completed at least three successful gait trails. A trial was considered "successful" when constant walking speed was obtained during gait.

Table 2-1 showed the 14 segmental landmarks that were digitized for capturing body motions. Trajectories of all the landmarks were recorded and filtered with a fourth-order, bidirectional Butterworth low-pass filter with a cutoff frequency of 10 Hz. Origins and definitions of each segmental coordinate system determined by the digitized segmental landmarks are listed in Table 2-2. The illustrations of each segmental coordinate system together with the placements of the digitized landmarks are also shown in Figure 2-4 and Figure 2-5.

The kinematic data were obtained by calculating the orientations of segmental coordinate system. The mass and inertial properties were individually calculated with reference to the coefficients from previous literature [39]. The kinetic data including

doi:10.6342/NTU201901683

joint force, moment, and power are analyzed by the methodology of inverse dynamics.

Table 2-1 Descriptions of the digitized segment landmarks for the right leg

Segment	Digitized Landmark	Description
Pelvis	RASIS	Right ASIS
	LASIS	Left ASIS
	SAC	Mid-point between the right and left PSISs
Right Thigh	RLFC	Right lateral femoral epicondyle
	RMFC	Right medial femoral epicondyle
	RGTO	Right greater trochanter
Right Shank	RLMA	Right lateral malleolus
	RMMA	Right medial malleolus
	RFIH	Right fibula head
	RTTR	Right tibia tuberosity
Right Foot	RRCA*	Right rear heel
	RLCA*	Right lateral heel
	RMCA*	Right medial heel
	RTOE	Right mid-point of 2^{nd} and 3^{rd} metatarsal heads

* Vertical coordinates of RRCA, RLCA, and RMCA at neutral position are equal

doi:10.6342/NTU201901683

Table 2-2 Origins and definitions of segmental coordinate system for the right leg

Segment	Origin	Definition
Pelvis	Right hip joint center (RHJC) determined by the method proposed by Bell et al. [40]	$\vec{X}$: The unit vector of the line passing from LASIS to RASIS
		$\vec{Y}$: The unit vector of the cross product of the $\vec{Z}$ and $\vec{X}$
		$\vec{Z}$: The unit vector superiorly normal to the plane containing RASIS, LASIS, and SAC
Right Thigh	Right knee joint center (RKJC) determined by the mid-point of RLFC and RMFC	$\vec{X}$: The unit vector of the line passing from RMFC to RLFC
		$\vec{Y}$: The unit vector anteriorly normal to the plane containing RGTO, RLFC, and RMFC
		$\vec{Z}$: The unit vector of the cross product of the $\vec{X}$ and $\vec{Y}$
Right Shank	Right Ankle Joint Center (RAJC) determined by the mid-point of RLMA and RMMA	$\vec{X}$: The unit vector of the cross product of the $\vec{Y}$ and the line passing from RAJC to RTTR
		$\vec{Y}$: The unit vector anteriorly normal to the plane containing RFIH, RLMA, and RMMA
		$\vec{Z}$: The unit vector of the cross product of the $\vec{X}$ and $\vec{Y}$
Right Foot	RRCA	$\vec{X}$: The unit vector of the cross product of the line passing from RRCA to RTOE and $\vec{Z}$
		$\vec{Y}$: The unit vector of the cross product of the $\vec{Z}$ and $\vec{X}$
		$\vec{Z}$: The unit vector superiorly normal to the plane containing RRCA, RLCA, and RMCA

doi:10.6342/NTU201901683

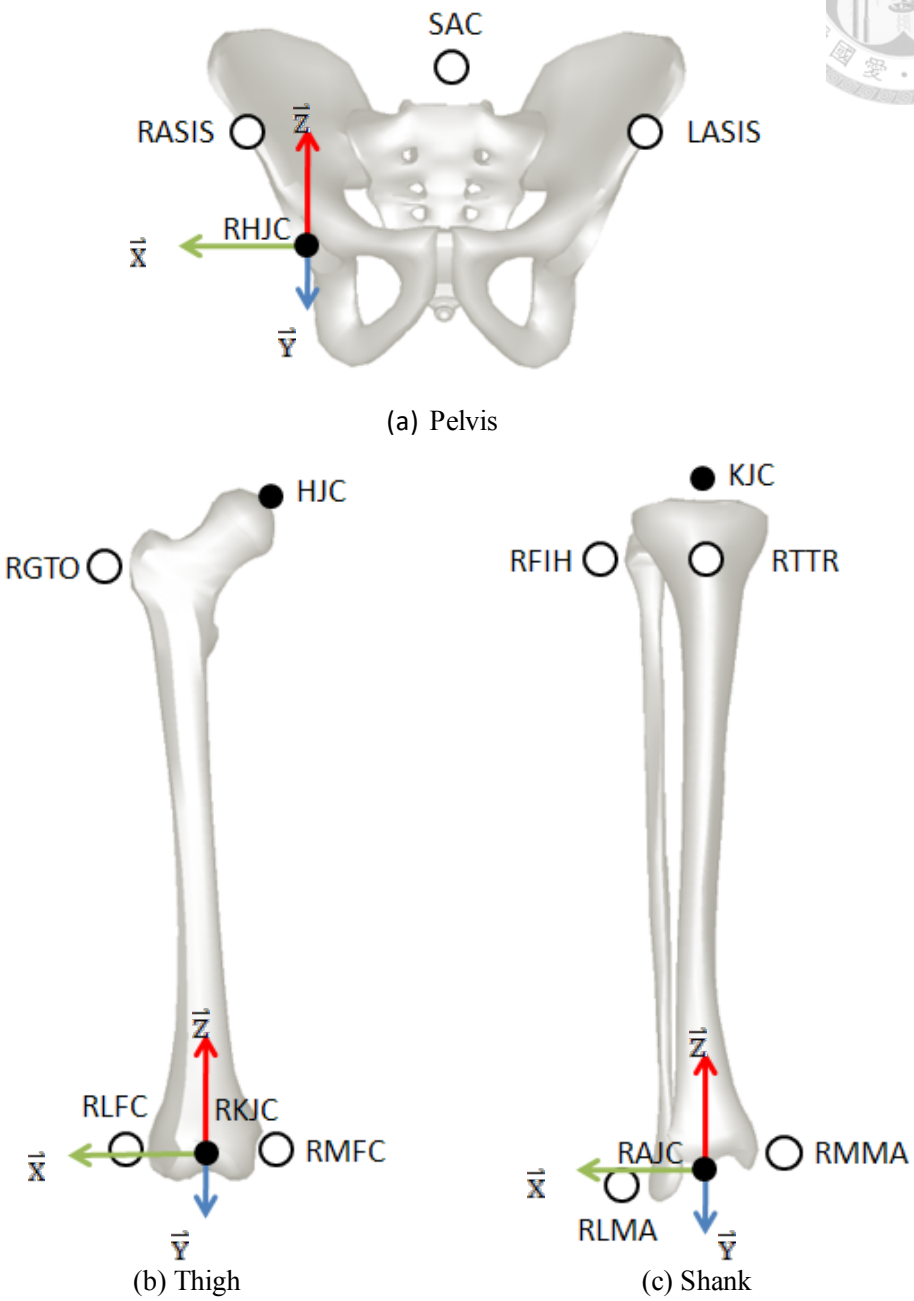

Figure 2-4 Illustrations of segmental coordinate systems and the digitized landmarks for the (a) pelvis, (b) right thigh, and (c) right shank in A-P view

doi:10.6342/NTU201901683

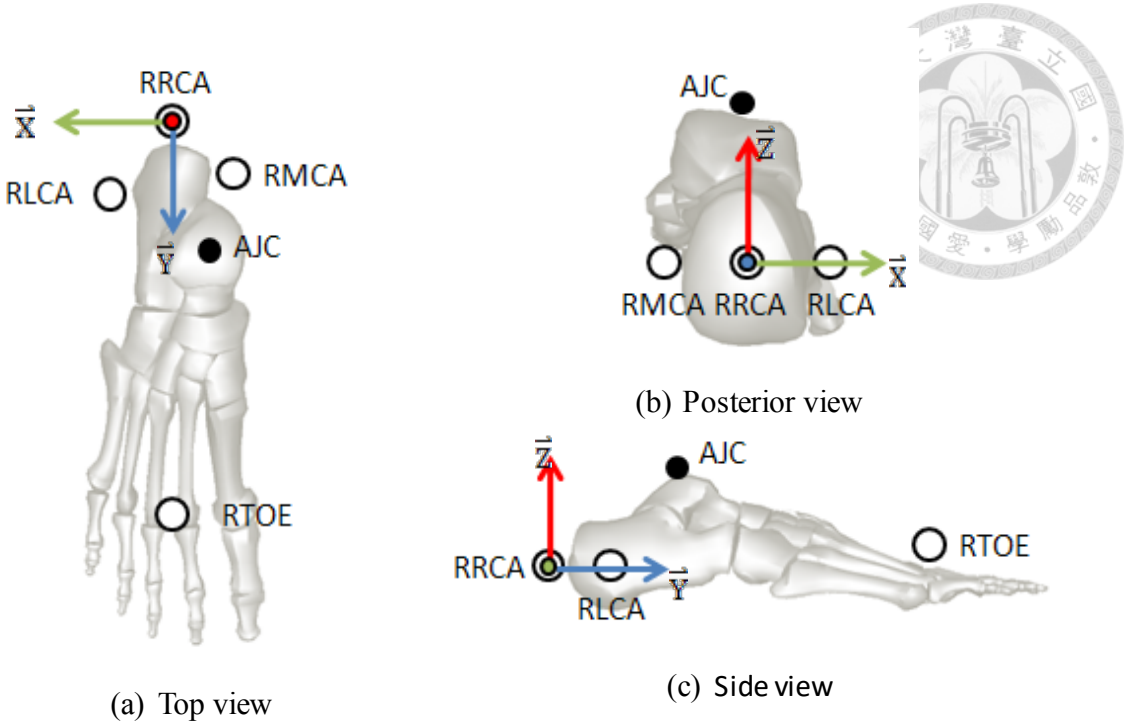

(a) Top view

(b) Posterior view

(c) Side view

Figure 2-5 Illustrations of segmental coordinate system and the digitized landmarks for the right foot in (a) top view, (b) posterior view, and (c) side view

doi:10.6342/NTU201901683

2.4 Energy Flow Model

The energy flow diagram likens potential and kinetic energy to a fluid, while body segments are likened to tanks that can store and release this fluid. The joints are likened to flow sources and sinks, and the mechanical work that transmits energy between body segments through joint forces and moments are like monoarticular pipes that the fluid flows through between the tanks, hence the term energy flow. The diagram can reveal the energy distribution over multiple segments, simultaneously.

2.4.1 Detailed energy flow diagram

A new symbolic convention of the detailed energy flow diagram which has four core elements, namely translational energy flow (TF) mediated by joint forces, rotational energy flow (RF) mediated by joint moments, segmental energy change rate, and joint power was proposed in this research. TF was calculated by TF $= F \cdot v_j$, whereas v_j is the linear velocity of a joint center and F is the joint force. TF is the power used to transmit the joint force while producing the translational movement in the direction of energy flowing across a joint. In a detailed energy flow diagram (Figure 2-6), the horizontal arrows that directly connect the body segments represent

doi:10.6342/NTU201901683

translational energy flow.

RF was calculated by $RF = M \cdot \omega_s$, whereas ω_s is the angular velocity of a segment and M is the joint moment. In a detailed energy flow diagram (Figure 2-6), the horizontal arrows connecting the segments through the joints represent the rotational energy flow. For either translational or rotational energy flow, a positive (negative) value represents an inflow (outflow) of energy to a segment. For either translational energy flow or rotational energy flow, the direction of a horizontal arrow is determined by the sign of the value obtained from energy flow analysis. For instance, the arrow direction of a positive energy flow shall be toward a segment, which also means the energy is flowing into the segment.

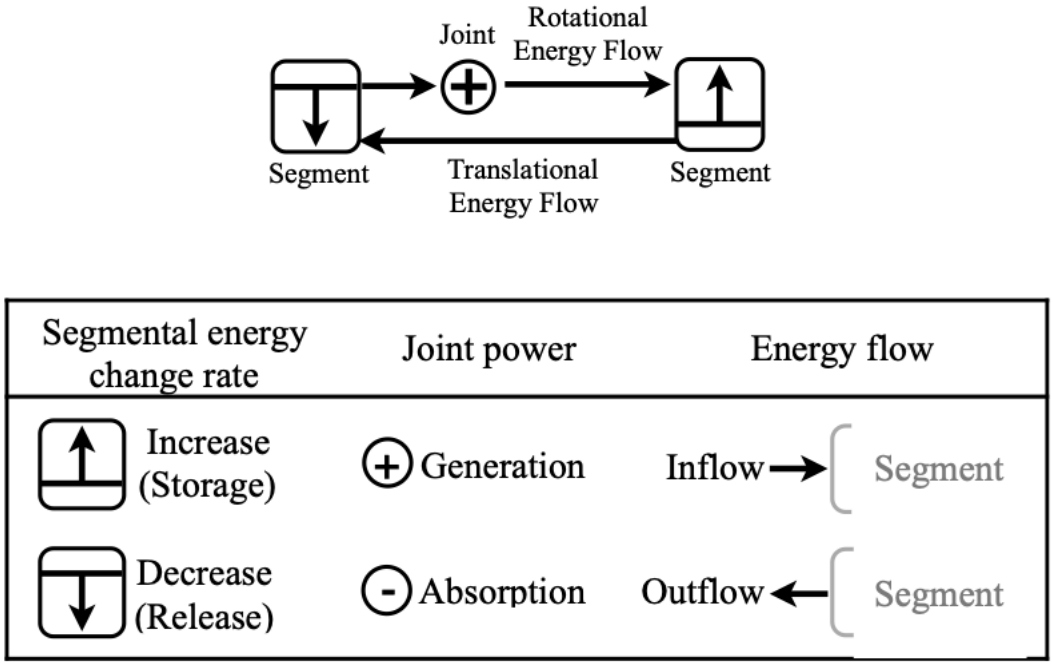

Figure 2-6 A new symbolic convention of the detailed energy flow diagram.

doi:10.6342/NTU201901683

The segmental energy change rate ($\dot{E}_s$) is for the change of the total mechanical energy of a segment. Total mechanical energy refers to the sum of potential energy (PE), translational kinetic energy (TKE), and rotational kinetic energy (RKE). PE was calculated by $PE = mgh$, whereas m is the mass of a segment, g is the gravitational acceleration, and h is the height of the center of mass of a segment. TKE was calculated by $E = \frac{1}{2} m v_s \cdot v_s$, whereas v_s is the linear velocity of a segment's center of mass. RKE was calculated by $KE = \frac{1}{2} \omega_s \cdot I \omega_s$, whereas I is the moment of inertia of a segment. In a detailed energy flow diagram (Figure 2-6), squares represent different body segments where the direction of a vertical arrow within a square is determined by the sign of the value of the corresponding segmental energy change rate. For example, the arrow direction of positive segmental energy change rate is upward, which also means that the segmental energy is increasing, i.e. energy storage.

Joint power (JP) was calculated by $JP = M \cdot \omega_j$ whereas ω_j is the angular velocity of a joint. The role of joint power is to modulate rotational energy flow across a joint. A positive (negative) joint power refers to power generation (absorption) by muscles. In our energy flow model, the joint power also equals to the sum of proximal RF of the distal segment and distal RF of the proximal segment, e.g., $JP_{knee} = RF_{shank,}$

doi:10.6342/NTU201901683

$_{proximal}$ + $RF_{thigh,\ distal}$. This equation can help to clarify the role of joint power on rotational energy flow. In a detailed energy flow diagram (Figure 2-6), circles represent joints, and '+' and '-' symbols indicate whether the joints generate (symbol: +) or absorb (symbol: -) energy.

By connecting ankle joint power with other energetic elements, the utilization of ankle power can be intuitively tracked within the proposed detailed energy flow diagram like a map, which further describes movement strategy of walking during ankle push-off.

doi:10.6342/NTU201901683

2.4.2 Simplified energy flow diagram

In order to ease the observation of the energy flow characteristics, the detailed energy flow diagram can be further simplified by merging translation energy flow and rotational energy flow into either segmental proximal flow ($\dot{E}_p$) or segmental distal flow ($\dot{E}_d$). The segmental proximal/distal flow was calculated by:

$$\dot{E}_p(or\ \dot{E}_d) = F \cdot v_j + M \cdot \omega_s$$

The segmental proximal/distal flow indicates the energy entering or leaving a segment at its proximal or distal part, which is easier to comprehend. Taking the thigh for example, the positive thigh proximal flow ($\dot{E}_{p,\,thigh}$) represents there is an energy inflow to the thigh at the hip joint, whereas the negative thigh distal flow ($\dot{E}_{d,\,thigh}$) represents there is an energy outflow from the thigh to the knee joint (Figure 2-7).

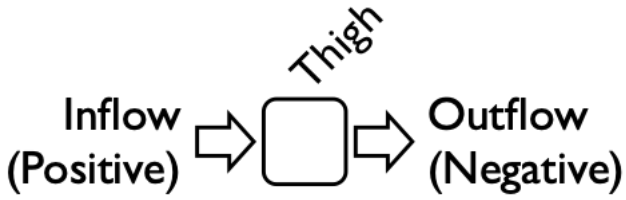

Figure 2-7 Segmental proximal and distal flows in a simplified energy flow diagram

doi:10.6342/NTU201901683

In a simplified energy flow diagram, the segmental energy change rate ($\dot{E}_s$) equals to the summation of segmental proximal and distal flows of a segment, i.e. $\dot{E}_s = \dot{E}_d + \dot{E}_p$. For example, 50 Watts of $\dot{E}_{p,thigh}$ and -20 Watts of $\dot{E}_{d,thigh}$ indicate that $\dot{E}_{s,thigh}$ increases 30 Watts (Figure 2-8). It allows us to look into the regulation of the segmental energy. Through this observation, we can study how the energy flow modulates the potential energy and kinetic energy of the segment.

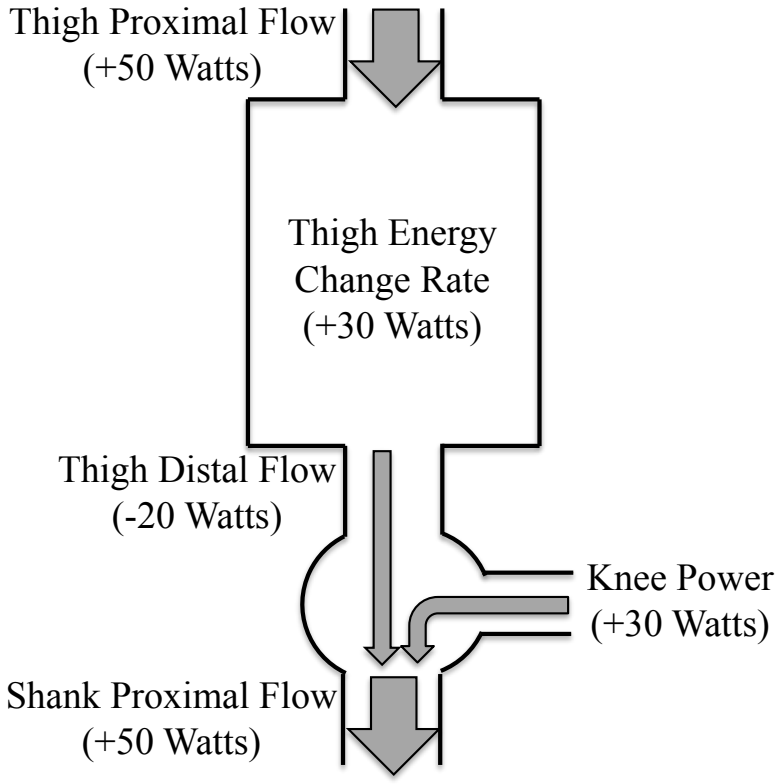

Figure 2-8 An example of a simplified energy flow diagram including the thigh and the knee joint.

doi:10.6342/NTU201901683

In a simplified energy flow diagram, a positive joint power can result in two kinds of flow pattern across the joint in terms of a pure energy source and increasing transferring energy. In contrast, a negative joint power can result in two kinds of flow pattern across in terms of a pure energy sink and decreasing transferring energy. The amount of power leaving the joint equals that entering the joint, i.e., the joint power equals to the summation of $\dot{E}_p$ of the distal segment and $\dot{E}_d$ of the proximal segment, e.g. $P_{knee} = \dot{E}_{p,shank} + \dot{E}_{d,thigh}$. For example, 50 Watts of $\dot{E}_{p,shank}$ and -20 Watts of $\dot{E}_{d,thigh}$ represent that the knee generates 30 Watts of power (P_{knee})(Figure 2-8).

Figure 2-9 showed another example of the energy flow characteristics presented by the energy distribution and flow pattern in a simplified energy flow diagram. It is effortless to conclude that the energy stored in the thigh and the shank is contributed by the power generation of knee muscle. The example demonstrates that the proposed energy flow model provides an intuitive way to observe joint power utilization. Otherwise, either the role of joint power or the source of segmental energy change may remain ambiguous if not bridging joint and segmental energetics together.

Another format of presenting the energy flow pattern of one leg was also adopted in this research in order to intuitively link to the movement (Figure 2-10). Since there

doi:10.6342/NTU201901683

is no foot distal flow during the swing phase, i.e. foot does not contact the ground, foot energy change rate is identical to the foot proximal flow. Accordingly, there are eleven energy flow elements in the swing leg model, including the pelvis distal flow, hip power, thigh proximal flow, thigh energy change rate, thigh distal flow, knee power, shank proximal flow, shank energy change rate, shank distal flow, ankle power, and foot proximal flow.

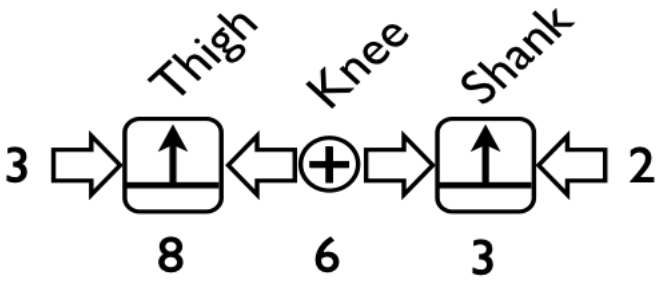

Figure 2-9 A simplified energy flow diagram to reveal the energy source of the thigh and the shank

doi:10.6342/NTU201901683

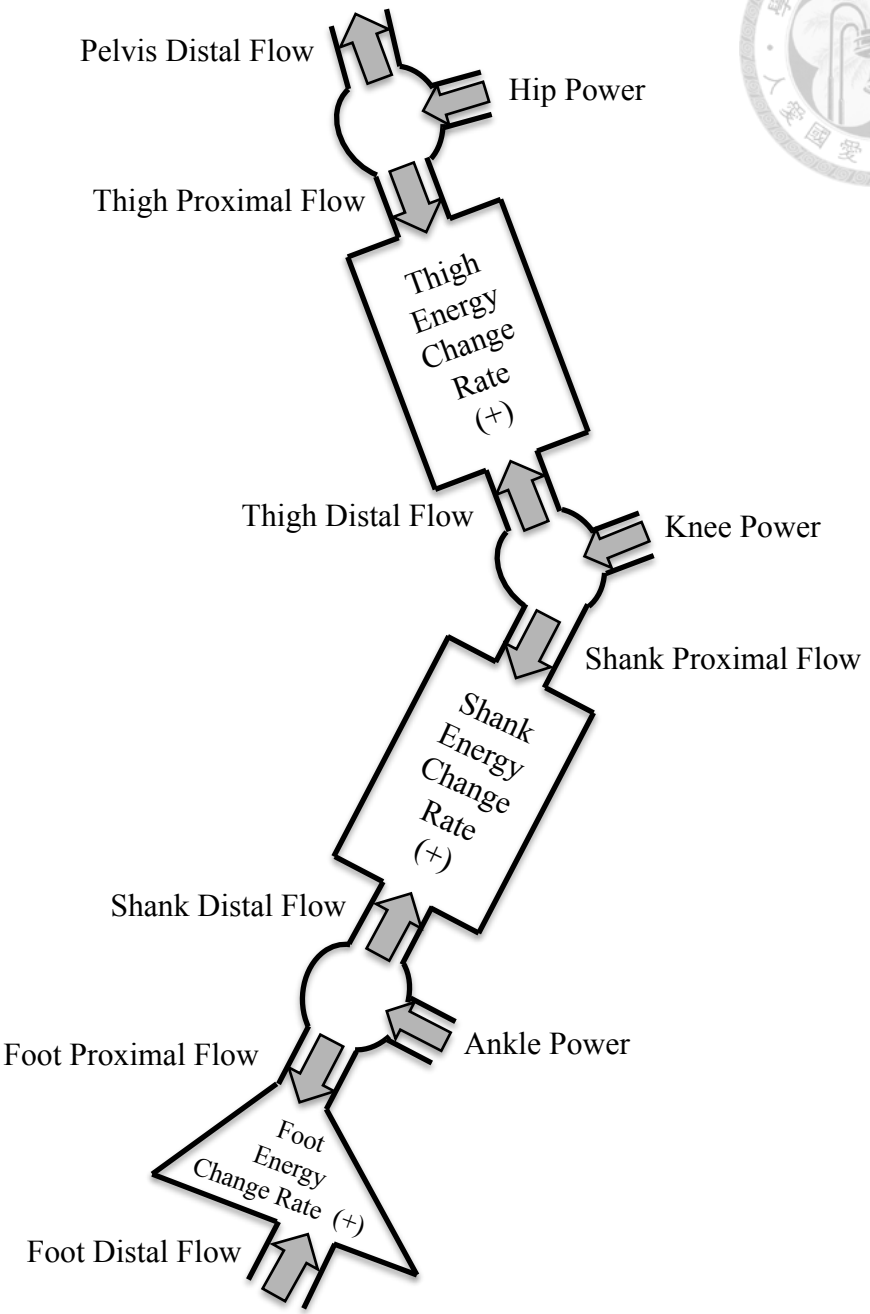

Figure 2-10 A complete simplified energy flow diagram of one leg. All energy flows are presented in the positive direction.

doi:10.6342/NTU201901683

2.5 Data Analysis

2.5.1 Construction of a detailed energy flow diagram at the instant of push-off

The translational energy flow, rotational energy flow, joint power, and segmental energy change rate were analyzed. Energy flow between the foot and ground were calculated based on techniques in the literatures that account for energy dissipated in foot deformation [41-43]. The detailed energy flow diagram was constructed at the instant of peak ankle power generation since such instant is considered representative of push-off phase [44-46]. Subsequently, the distribution of ankle power generated during push-off was further investigated by analyzing the mechanical energy of each segment. These analyses were performed to reveal how ankle power was utilized and to test whether the ankle power generated during push-off delivered substantial propulsive energy to the pelvis.

2.5.2 Factor analysis of the energy flow characteristics in swing phase

The kinematic data that was used to calculate the energy flow were normalized to the duration of the swing phase (yielding the relative time profiles between 0% and 100%) and were averaged over the three recorded trials. The energy flow data of all

doi:10.6342/NTU201901683

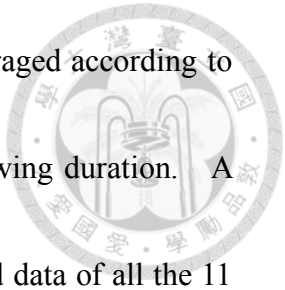

subjects were then normalized to the subject's body mass, and averaged according to the normalized time profiles at 1 percent interval along with the swing duration. A correlation coefficient matrix derived from the normalized averaged data of all the 11 energy flow elements in the swing leg model would be produced to evaluate the correlation between each of the energy flow element. The correlation coefficient ranges from 0 to 1 and the higher coefficient indicates the greater correlation. The correlation matrix would be used as inputs for the factor analysis. By rotating the principal components, factor analysis is then utilized to extract the characteristics of a high-dimensional dataset. The extracted 1st and 2nd factors indicate the first two most prominent energy flow patterns of the entire swing phase. For each factor, energy flow elements with significant absolute loadings (> 0.8) would further be depicted in the energy flow model while the sign of the loading determined the flow direction of the corresponding energy flow element. Consequently, the energy flow characteristics of the swing leg can be intuitively observed corresponding to each of the extracted factors. The independent t-test was used to compare the walking speeds between the young adults and the elderly.

doi:10.6342/NTU201901683

2.5.3 Verification of the proposed energy flow analysis

This research has developed a software program to perform the proposed energy flow analysis (Figure 2-11). Nevertheless, it would be difficult to judge the robustness of the data if the accuracy of our energy flow analysis technique was not verified. Our energy analysis technique was verified by comparing the segmental energy change rates calculated from kinematic data with the summation of the corresponding energy inflow/outflow that are calculated via inverse dynamics. Since the segmental energy change rate was analyzed via simple calculations, it was less prone to error. Thus, the accuracy of developed technique can be assured if the results from both calculations are similar. In previous literatures, the discrepancy between these two calculating methods was called power imbalance. Theoretically, the power imbalance is zero since either calculation follows the principles of rigid-body dynamics.

Figure 2-12 showed the segmental energy change rates of thigh, shank, and foot from a gait trial of a young healthy adult, in which data is processed by our developed software. The results showed that each segmental energy change rate was highly matched with the summation of the corresponding energy inflow/outflow. Since nearly zero power imbalance was achieved, the accuracy of developed technique was

doi:10.6342/NTU201901683

assured. Another comparison of segmental energy change rates cited from the other research [47] was showed in Figure 2-12 for reference.

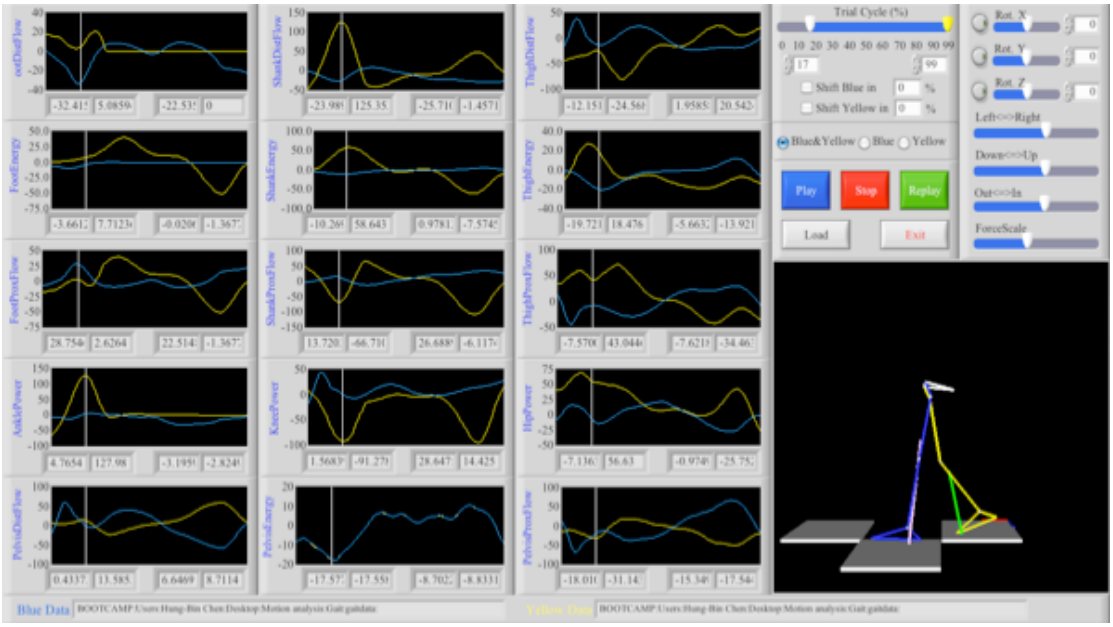

Figure 2-11 The user interface of the developed energy flow analysis software. Chart and value of each energy flow within the proposed model can be conveniently assessed via the software. In addition, 3D animation of gait is shown together with ground-reaction-forces in order to distinguish which gait event is being analyzed.

doi:10.6342/NTU201901683

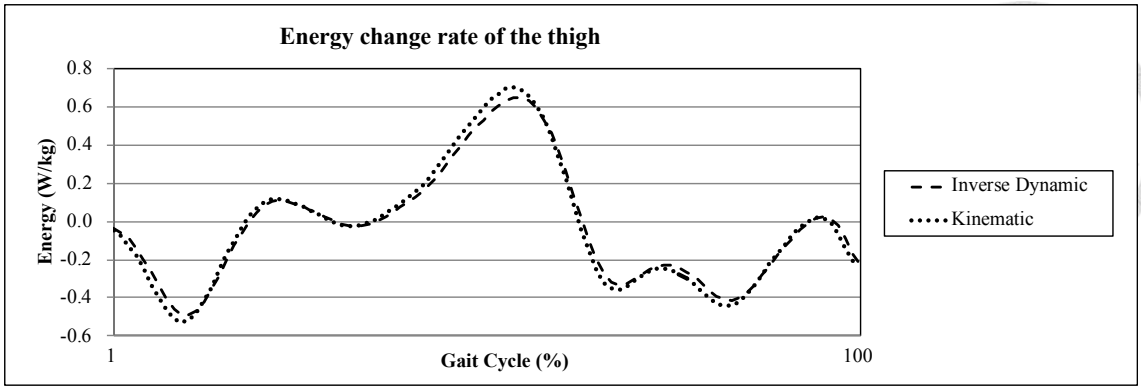

(a)

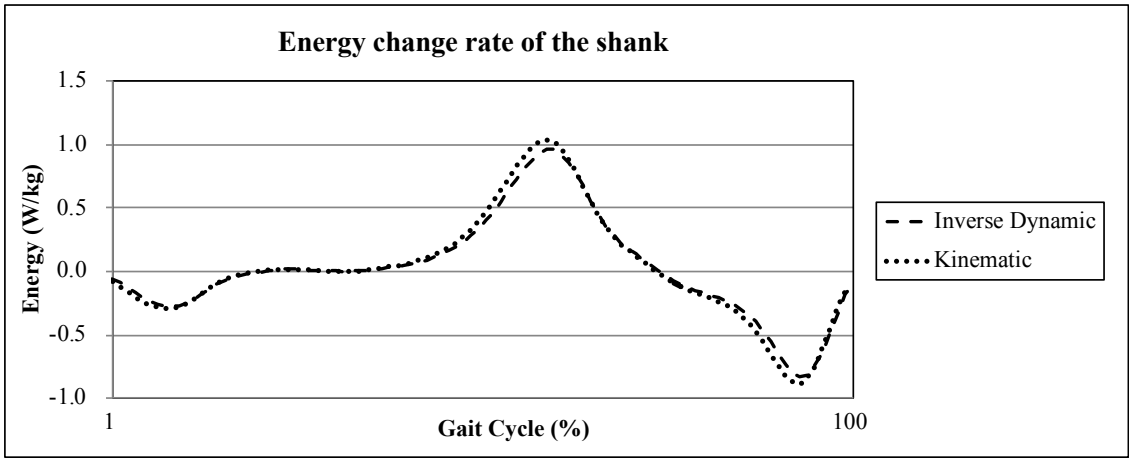

(b)

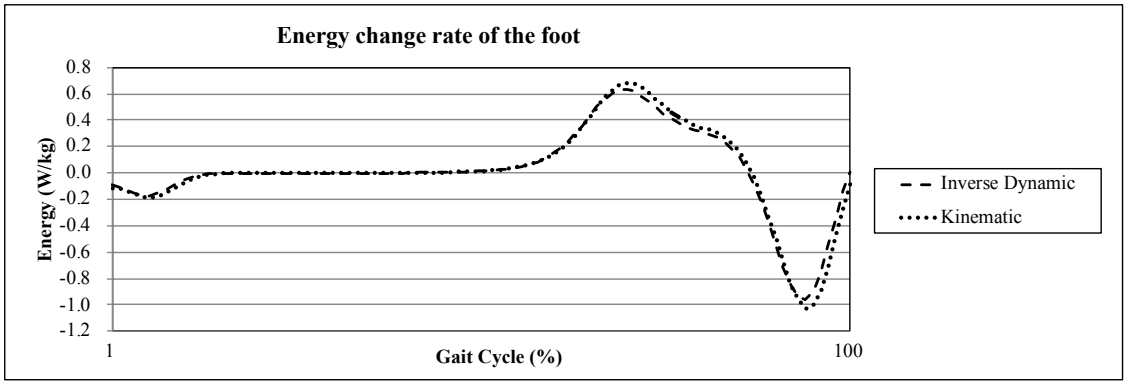

(c)

Figure 2-12 Segmental energy change rate of (a) thigh, (b) shank, and (c) foot calculated by inverse dynamics (dash-line) and kinematic data (dot-line). Charts from both calculations were highly matched, i.e. nearly zero power imbalance.

doi:10.6342/NTU201901683

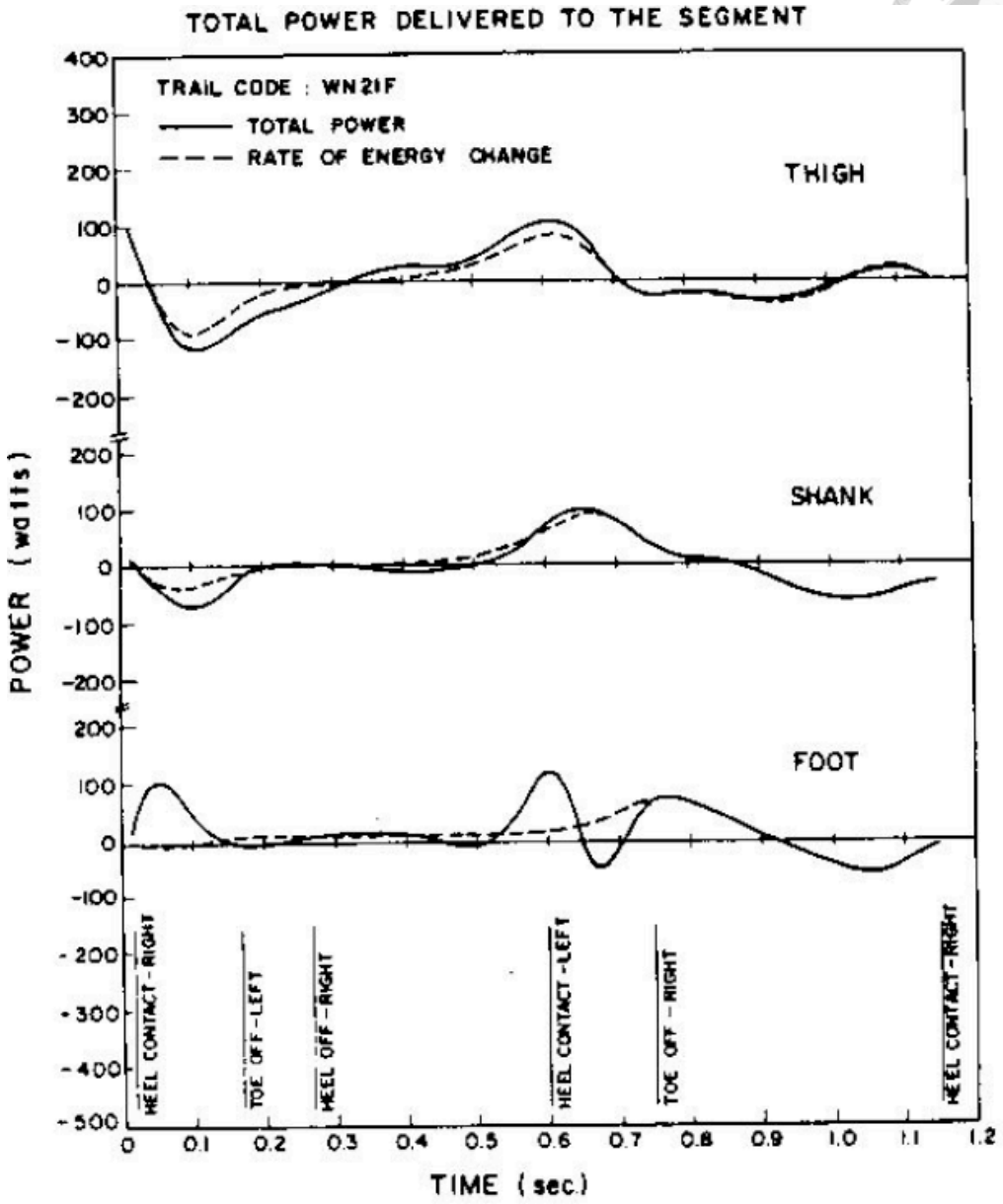

Figure 2-13 Comparison of segmental energy change rates cited from the other research [47]. Considerable power imbalance existed in the stance phase for all segments whereas nearly zero power imbalance in the swing phase.

doi:10.6342/NTU201901683

Chapter 3

Mechanical energy utilization of ankle push-off in young adults

3.1 Detailed energy flow diagram during ankle push-off

The gait data for this clinical application of energy flow analysis were collected at self-selected speeds (1.43±0.09 m/s) from 8 healthy young adults (Age: 23±2 years old, Gender: male). The energetic data obtained from the developed energy flow model (Appendix II) were used to construct the detailed energy flow diagram at the moment of peak ankle power generation (Figure 3-1).

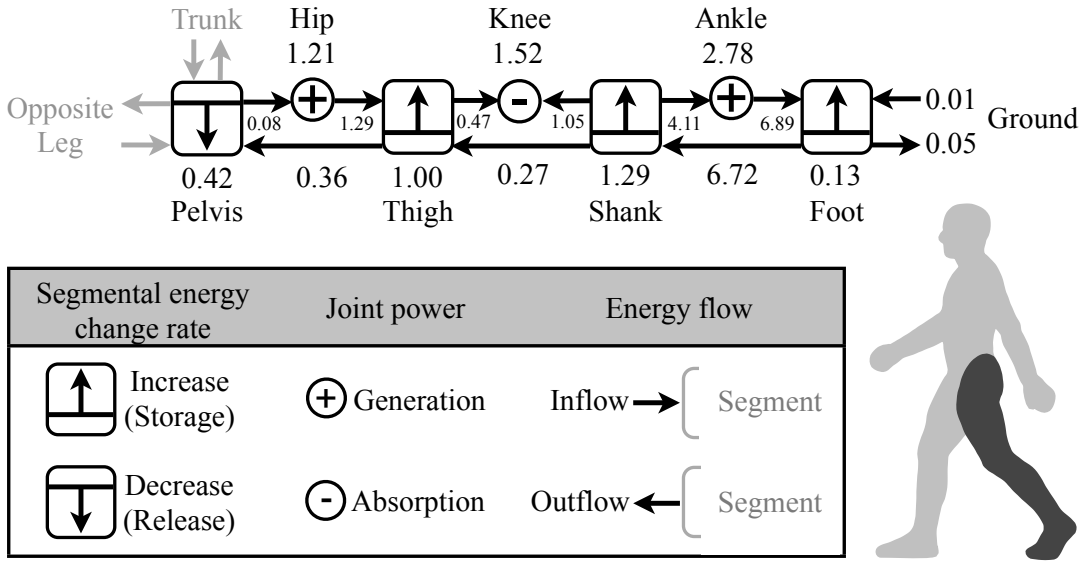

Figure 3-1 A detailed energy flow diagram at the peak of ankle power generation during push-off. All values are reported in power normalized by body weight (W/kg) either above or below their corresponding symbol. Reported values are the average across subjects.

doi:10.6342/NTU201901683

3.2 Energy flow between the shank and the foot

There was an energy flow loop between the shank and the foot where energy moved from the shank to the foot through rotational energy flow as well as where energy moved back to the shank from the foot through translational energy flow (Figure 3-1). Within the loop, the ankle power (2.78±0.22 W/kg) joined the rotational energy outflow from the shank (4.11±0.80 W/kg) and produced an augmented energy inflow to the foot of 6.89±1.06 W/kg. A small portion of this augmented energy flow powered the motion of the foot (0.13±0.04 W/kg), and even less of that was transmitted to the ground (0.05±0.22 W/kg). However, the majority of this augmented energy was transmitted to the shank through translational energy flow (6.72±0.96 W/kg). In other words, this translational energy flow was transformed from the rotational energy flow induced by ankle muscles as shown in the energy flow loop. The energy flow loop between the shank and the foot is the energetic representation of ankle plantarflexor moment (producing rotational power) inducing the upward ankle reaction force (producing translational power) on the shank through the lever action of the foot.

doi:10.6342/NTU201901683

3.3 Utilization of ankle power

The detailed energy flow diagram (Figure 3-1) shows how energy moved from the lower leg segments all the way up to the pelvis through translational energy flow, which could be considered the "push-off" power. However, we found that the magnitude of translational energy flow moving from the shank to the thigh (0.27±0.51 W/kg) was only about 10% of the ankle power (2.78±0.22 W/kg). The majority of ankle power either increased the mechanical energy of the shank (1.29±0.24 W/kg, about 46%) or was absorbed by the knee (1.05±0.51 W/kg, about 38%). The remaining ankle-induced power moved from the shank to the thigh through translational energy flow (0.27±0.51 W/kg) and was combined with power generated from the hip (1.29±0.34 W/kg) to increase the mechanical energy of the thigh (1.00±0.19 W/kg). Although the translational energy flow from the thigh to the pelvis (0.36±0.61 W/kg) transmitted some of the ankle joint power to the pelvis, the detailed energy flow diagram (Figure 3-1) clearly illustrates how the majority of power generated by the ankle during push-off flowed to the ipsilateral leg and how little of that was transmitted toward the trunk.

doi:10.6342/NTU201901683

3.4 Energy flow of the pelvis

The utility of the energy flow diagram is that it graphically reveals the flow of energy through the entire leg, rather than focusing on a single joint or segment. However, one energy flow diagram only represents one instant at a time. In order to verify that our results are not unique to this single instant, we examined the translational energy flow from the trailing thigh to the pelvis during the entirety of push-off (Figure 3-2). We found that the translational energy flow applied to the pelvis was small compared to ankle power, and that energy only flowed into the pelvis for less than a half of the duration of push-off. We also examined the rotational energy flow between the pelvis and trailing thigh, and found that a small amount of energy was consistently flowing from the pelvis to the hip during the entirety of push-off (Figure 3-2).

doi:10.6342/NTU201901683

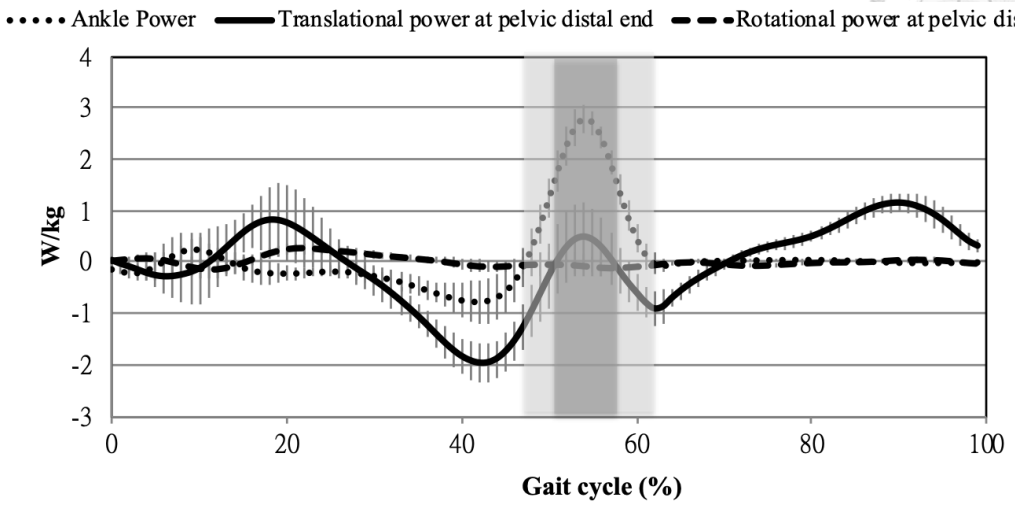

Figure 3-2 Ankle power and the energy transmitted to the pelvis. The light gray area indicates the period of push-off and the dark gray area indicates the duration of the translational energy inflow (positive value) to the pelvis. Standard deviations are shown as vertical bars. It can be observed that how much power generated by the ankle during push-off and how little power transmitted to the pelvis.

doi:10.6342/NTU201901683

3.5 Segmental energetics

To better understand the utilization of ankle power generated during push-off, we assessed the energy compositions of each segment in terms of potential energy and kinetic energy (Figure 3-3a-3d). The change in the total mechanical energy of the pelvis (-0.0222 J/kg) before and after push-off (Figure 3-3a) were dominated by the change in kinetic energy (-0.0225 J/kg). Furthermore, we found that such change in kinetic energy was largely determined by the change of the translational kinetic energy (-0.0225 J/kg), especially in the anterior-posterior direction (-0.0223 J/kg), while the change in rotational kinetic energy was several orders of magnitude smaller (<0.0001 J/kg) (Figure 3-3e).

doi:10.6342/NTU201901683

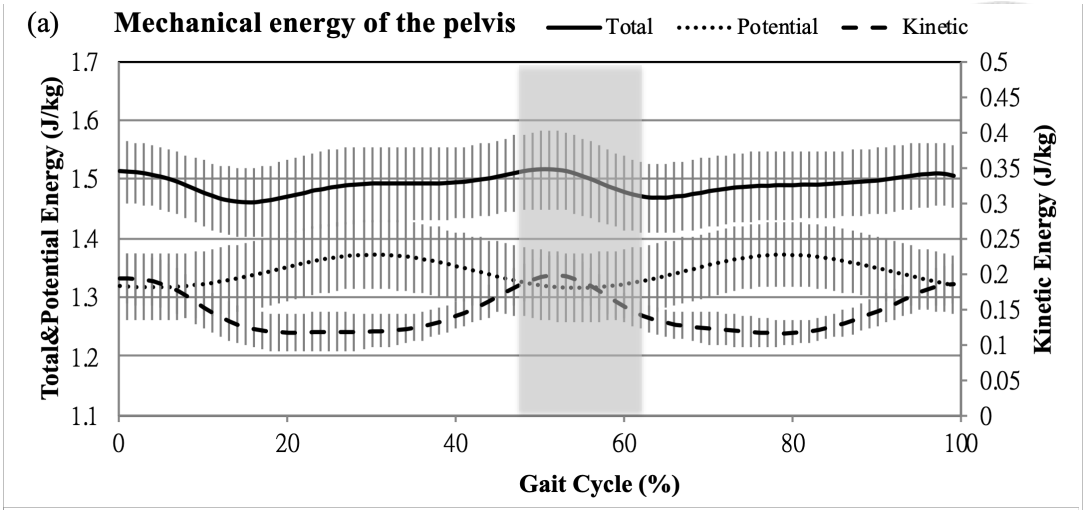

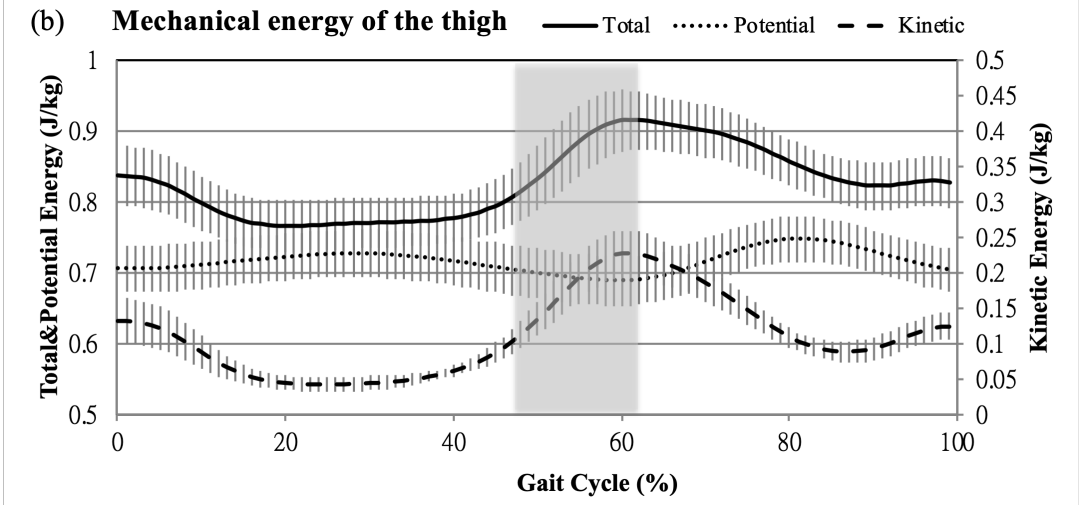

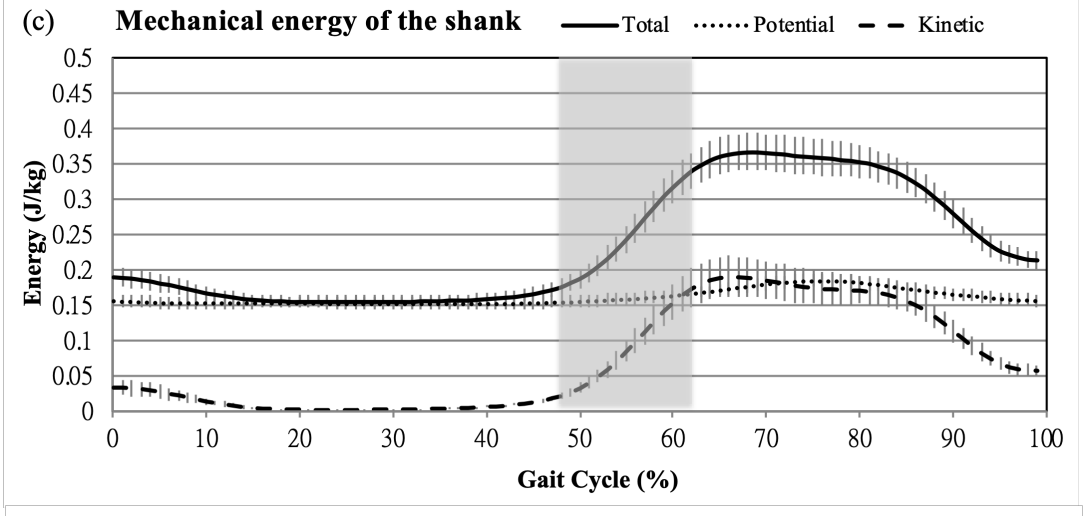

doi:10.6342/NTU201901683

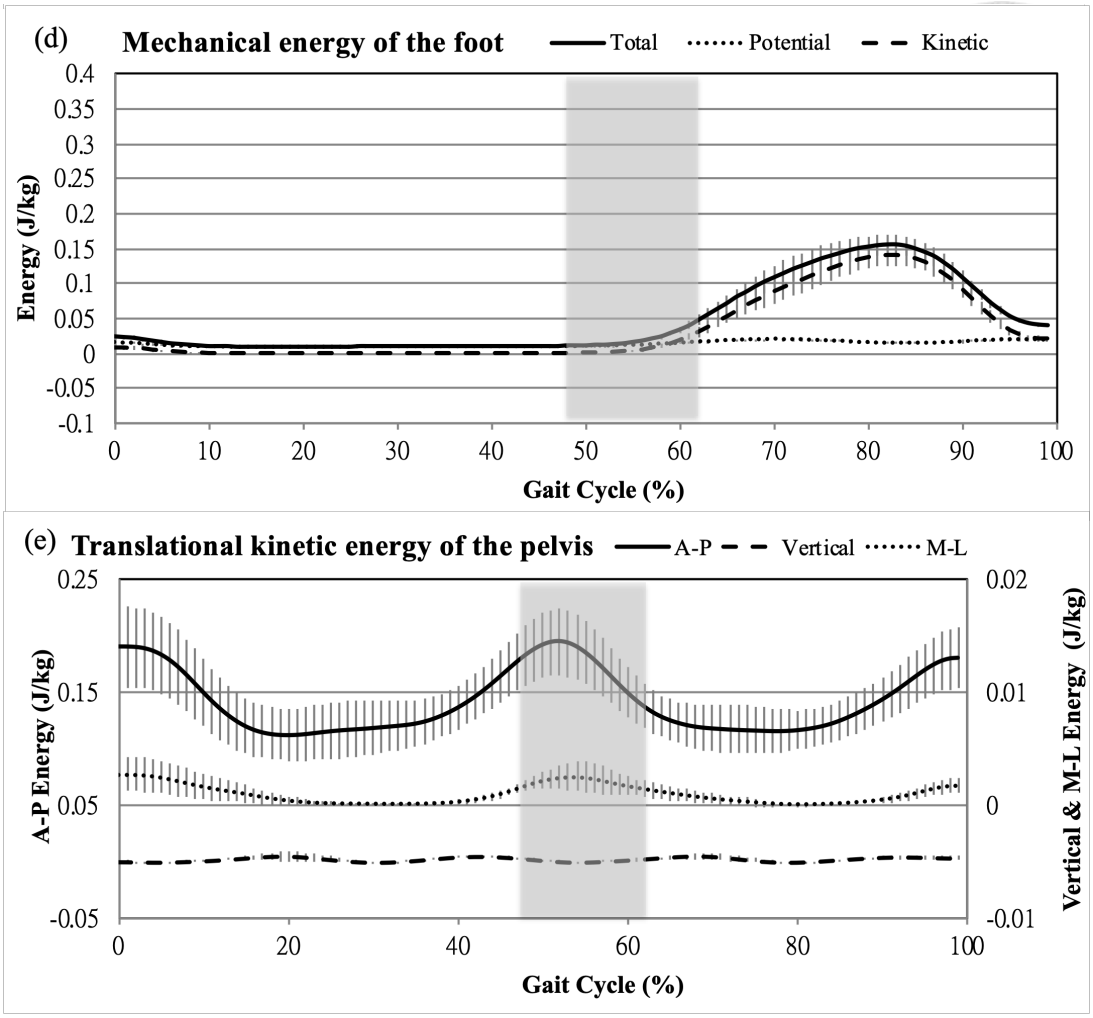

Figure 3-3 Energy characteristics of human gait. (a)-(d) The mechanical energy compositions of the pelvis, thigh, shank, and foot, respectively. (e) The composition of translational kinetic energy of the pelvis in terms of the anterior-posterior (A-P), medial-lateral (M-L), and vertical directions. The light gray area indicates the period of push-off. Standard deviations are shown as vertical bars.

doi:10.6342/NTU201901683

3.6 Discussion

At the instant of ankle peak power generation, our energy flow diagram showed that the ankle power was an important source of power for the motion of the ipsilateral leg. The ankle power supplied most of the energy required by the foot (0.13±0.04 W/kg) in the form of the rotational energy flow since another energy inflow from the ground was relatively small (0.01±0.03 W/kg) (Figure 3-1). We also found that the ankle power transformed into translational energy flow (6.72±0.96 W/kg) at the ankle joint, and such translational energy flow was the sole energy inflow to supply the energy required for the motion of the shank (Figure 3-1). As for the thigh, the hip-induced rotational energy flow (1.29±0.24 W/kg) and the translational energy flow (0.27±0.51 W/kg) from the shank were both energy sources (Figure 3-1). Our study gives a clinical application on how to use the energy flow diagram with the proposed convention to link joint energetics to segment energetics so that the movement strategy can be further explained. Since most of the ankle power supplies energy to ipsilateral foot, shank, and thigh, it can be readily inferred that the ankle power generated during push-off mainly propels the trailing leg forward as it transitions from stance to swing phase.

doi:10.6342/NTU201901683

The purpose of examining pelvic energetics was to assess the role played by ankle power on forward propulsion. Based on the kinematics, we calculated that the mechanical energy of the pelvis decreased (0.42±0.24 W/kg) at the moment of peak ankle power (Figure 3-1), and such decrease was largely determined by a decrease in kinetic energy (Figure 3-3e), indicating that the upper body is decelerating during push-off. Furthermore, we found that the trailing leg only performed positive work on the pelvis for less than half of the push-off period (Figure 3-2) and the net work performed by the trailing leg on the pelvis during the push off period was negative. The positive power supplied by the trailing leg was not enough to prevent the mechanical energy of the pelvis from decreasing during push-off (Figure 3-3a). The positive work performed by the trailing leg may mitigate some of the energy lost during double-limb support, but such does not contribute to a net increase in kinetic energy which is often associated with forward propulsion. Based on the distribution of power throughout the trailing leg and the relatively small amount of energy transferred to the pelvis, it implies that the primary role of ankle during push-off is to propel the trailing leg forward rather than deliver substantial propulsive energy to the pelvis.

Our study analyzed the utilization of ankle power generated during push-off by

doi:10.6342/NTU201901683

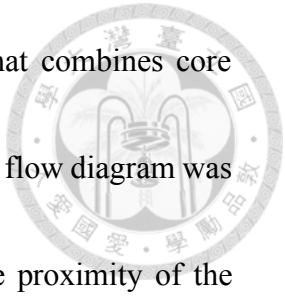

illustrating energy flow diagram in a new symbolic convention that combines core mechanical energetic elements together. Another schematic energy flow diagram was used previously [1]; however, the choice of symbols and the close proximity of the different symbols as well as numbers made identifying the different quantities and the direction of rotational energy flow difficult. The regular structure of our diagram eliminates such confusion; our symbolic convention clearly and readily shows where energy is increasing, where it is transferred to, and where it is generated or absorbed. Our symbolic convention in the diagram facilitates the conceptualization of mechanical energy transfer between body segments as water flowing through a system of pipes, storage tanks, and pumps. Such comparison allows readers use their understanding of a more familiar system and fluid flow to intuit energy transfer within the body. In addition, it eases the interpretation of energy flow analysis, especially when comparing energy flow characteristics of different movements or subject groups. Comparing energy flow patterns of various gait events between the able-bodied and patients with neuromuscular disorders would require numerous energy flow diagrams lining up together in order to discern the movement strategy. We expect that the symbolic convention in the energy flow diagram can give a more succinct and standardized

doi:10.6342/NTU201901683

representation than the previous diagram.

Another benefit of the symbolic convention in the energy flow diagram compared to alternative energy analysis techniques [18, 48] is the ability to show where and how energy has been transmitted during a movement, especially for the energy flow across adjacent segments. Thus, current techniques allow us to better explore the role of ankle during push-off in relation to other segments to be analyzed. For example, the ankle power generated during push-off can be tracked to demonstrate the power utilization shown in the energy flow diagram, which provides evidences to support previous studies that suggested the role of the ankle during push-off primarily contributes to the initiation of swing [16–19]. A previous study also yielded similar results in the push-off period which claimed that the power was generated at the hip and the ankle, absorbed at the knee, and very little was transferred to the trunk [1]. However, the joint power magnitudes of the knee and the hip from the previous study [1] were much smaller than those of this study partly since the previous study performed the analysis at some point in late push off, while our analysis was carried out at peak ankle power generation. Differences in equipment may also account for the discrepancy, as the contemporary digital 3D motion capture used in this study is more

doi:10.6342/NTU201901683

precise than the hand digitizing of markers from cine film, which was used in the previous study [1]. Differences are also attributed to the fact that our research took the energy dissipated in foot deformation into account. Our reported values of joint power compare better with those from a more recent investigation [5] than those from the previous study [1].

Several limitations of this research should be addressed in the future. Calculations of joint center velocity differ slightly between proximal and distal segments, which results in a discrepancy in the translational energy flow between those segments. The only discrepancy with significant figures was a 0.27 W/kg difference in the translational energy flow between the proximal shank and the distal thigh. Nevertheless, this discrepancy does not affect our findings since the direction of the translational energy flow from the shank to the thigh is consistent between the proximal shank and distal thigh. Therefore, in order to simplify the diagram, we only show the translational energy flow values calculated from the proximal end of the segments. Regardless of the source of such energy flow discrepancy is from the physical translation within the joint or the limitations of rigid body assumptions [49], a more recent study has found that taking account of the energy flow discrepancy can better

doi:10.6342/NTU201901683

capture energy changes of the body [48].

Another limitation of this study is that only the energy flow of trailing leg was presented. Nevertheless, ignoring the energy flow of the leading leg does not affect our results on the pelvis energetics even if the leading leg transmits energy to the pelvis during push-off due to the fact that we calculate the mechanical energy of the pelvis by pelvis kinematics only. In addition, the validity of the energy flow analysis has to be rigorously checked before applying to other areas such as sports or rehabilitation medicine, given our analysis was performed on the basis of limited number of healthy subjects. In order to give a more comprehensive example of applying our new symbolic convention, a future work of the whole body energy flow diagram at different gait phases is warranted.

doi:10.6342/NTU201901683

Chapter 4

Comparisons of swing energy flow characteristics between the young adults and the elders

Ten healthy elderly (mean age: 68.1±6.4 years; 5 females and 5 males) who could walk without any assistance or aids, and ten healthy young adults (mean age: 25.1±1.6 years; 2 females and 8 males) participated in this study. For both subject groups, the fast walking speed (1.77±0.15 m/s for the young adults, and 1.56±0.20 m/s for the elderly) was significantly faster ($p<0.05$) than the self-selected walking speed (1.15± 0.24 m/s for the young adults, and 1.11±0.18 m/s for the elderly). The young adults walked significantly faster ($p=0.012$) than the elderly at the fast walking speed, while not at the self-selected walking speed.

4.1 Mean profiles of the energy flow data in swing phase

Mean profiles of all subjects in terms of the energy flow data of the entire lower extremity during the whole swing phase was shown in Figure 4-1, including the energy flow profiles of the thigh in the four conditions as the young adults at the self-selected walking speed (Figure 4-1a) and at the fast walking speed (Figure 4-2b) as well as the

doi:10.6342/NTU201901683

elderly at the self-selected walking speed (Figure 4-1c) and at the fast walking speed (Figure 4-1d), the energy flow profiles of the shank (Figure 4-1e-1h), and those of the foot (Figure 4-1i-1l). In general, the fluctuation trends of the eleven energy flow elements along the swing phase were analogous in all the four conditions. Nevertheless, it was noted that there were great energy fluctuation and great variations among the subjects especially in the elderly at the fast walking speed.

As a representative pattern in the condition of the young adults at the self-selected walking, the early stage of the swing phase showed a negative pelvis distal flow, positive hip power, positive thigh proximal flow, and positive thigh energy change rate (Figure 4-1a). In addition, there were negative thigh distal flow, insignificant knee power, positive shank proximal flow, and positive shank energy change rate (Figure 4-1e). There were also negative shank distal flow and positive foot proximal flow (Figure 4-1i). During the late stage of the swing phase, only the pelvis distal flow, thigh distal flow, and shank distal flow were positive. The rest of the energy flow elements were all negative. The magnitude of ankle power was especially close to zero during the entire swing phase.

doi:10.6342/NTU201901683

(a)

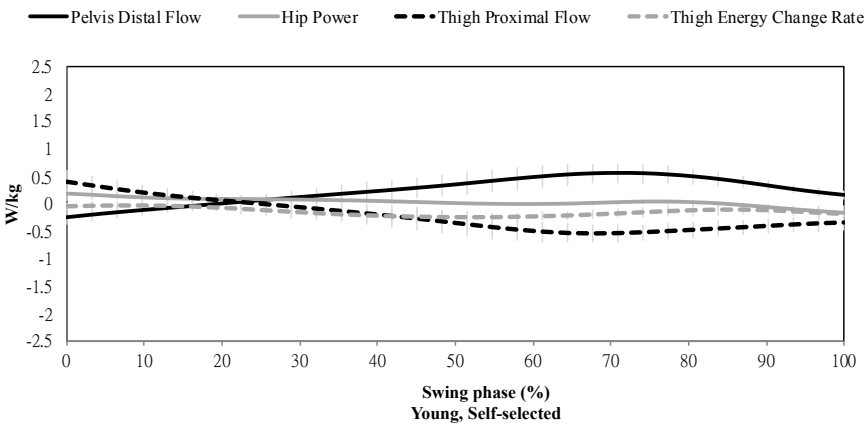

(b)

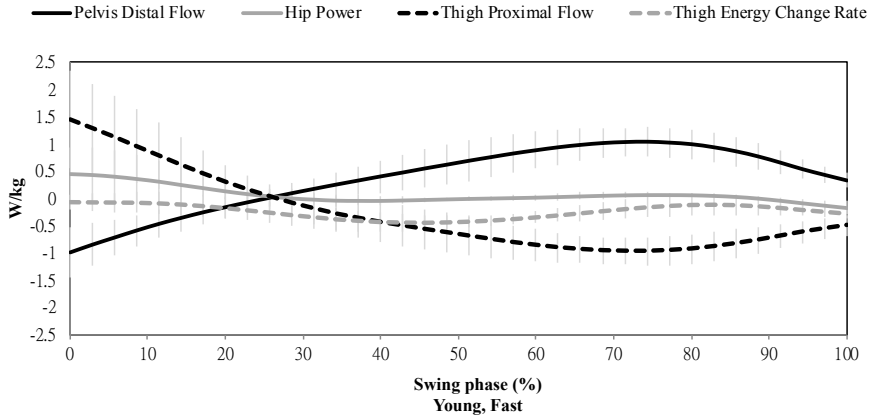

(c)

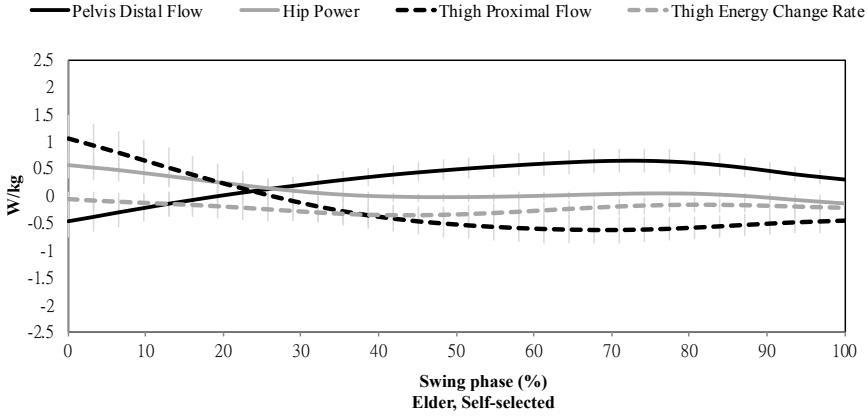

(d)

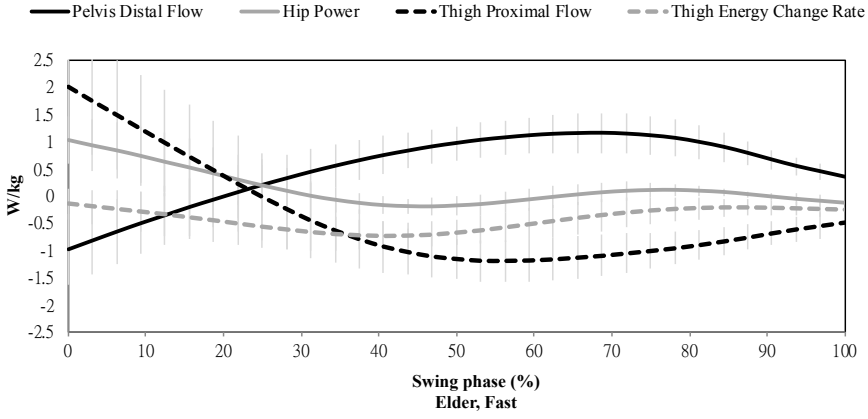

doi:10.6342/NTU201901683

(e)

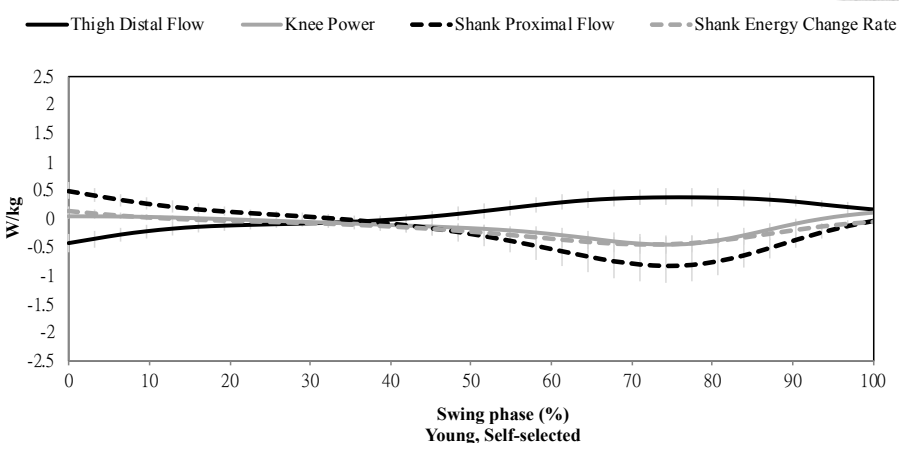

(f)

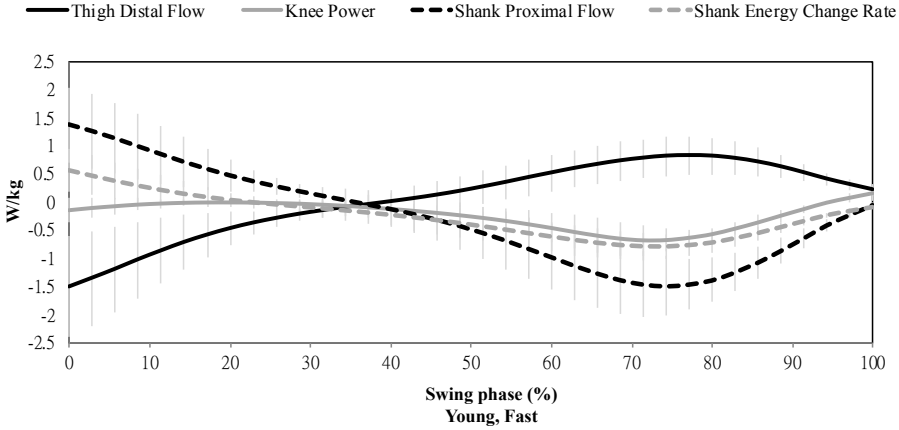

(g)

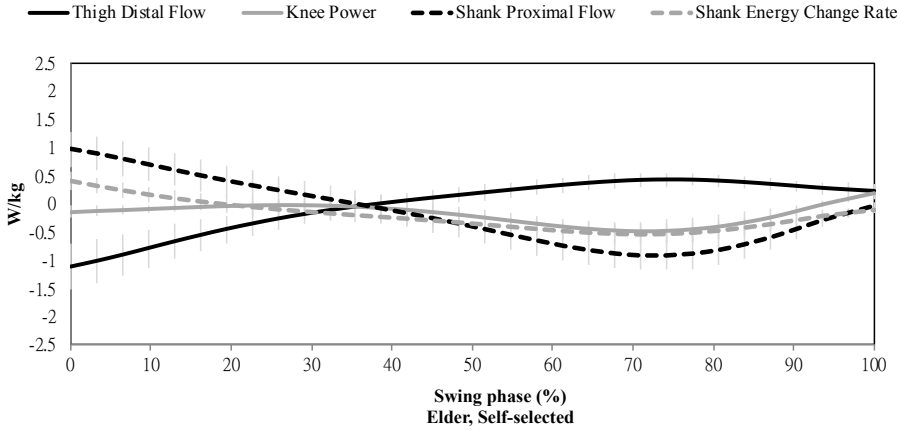

(h)

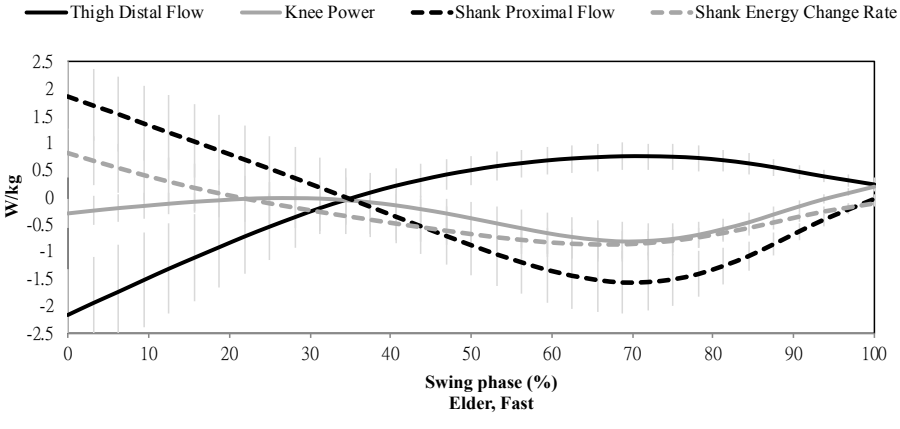

doi:10.6342/NTU201901683

(i)

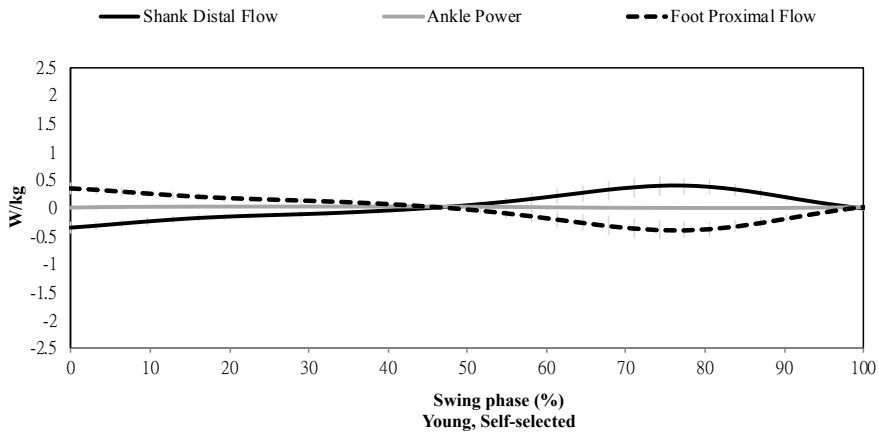

(j)

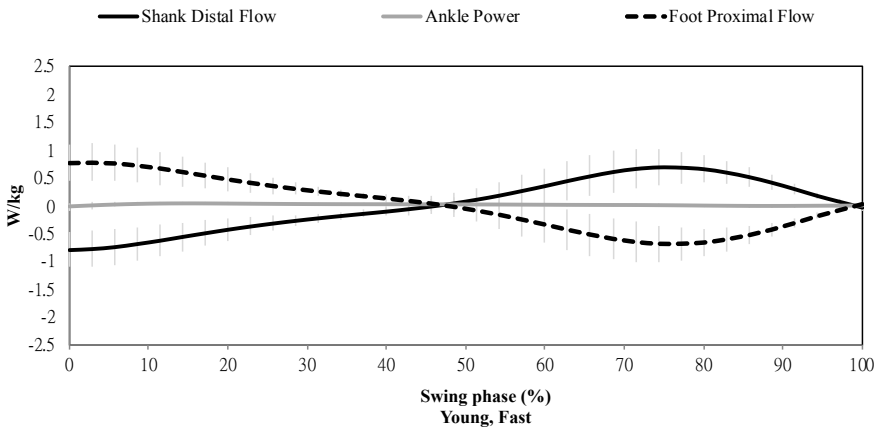

(k)

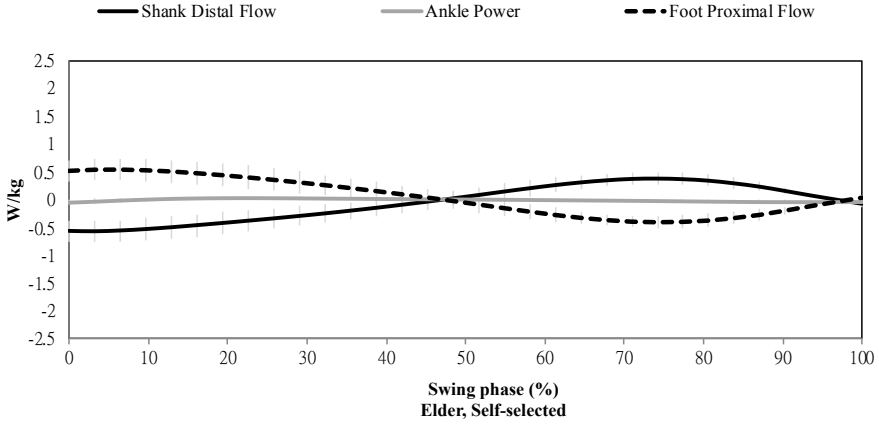

(l)

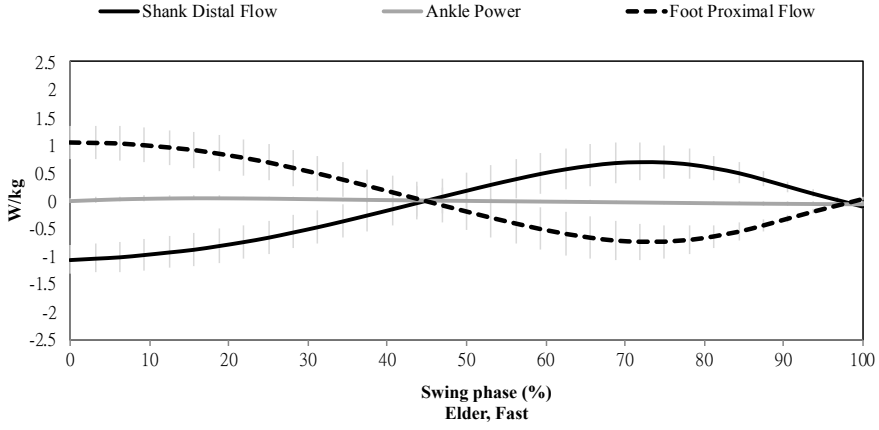

doi:10.6342/NTU201901683

Figure 4-1 Mean energy flows throughout the whole swing phase in the young adults and the elderly at the self-selected and fast walking speeds. Positive segmental proximal/distal flow represents that the energy flows into the corresponding segment. Positive joint power represents power generation.

doi:10.6342/NTU201901683

4.2 Factor analysis on energy flow mean profiles in swing phase

The complete correlation matrix of the energy flow elements covaried with each other was shown in Table 4-1. Notably, the correlation coefficients of ankle power were mostly smaller than 0.1 that could hardly influence the energy flow of the adjacent segments and joints. The ankle power was accordingly excluded in the subsequent analysis. By applying the factor analysis technique, the 1st and 2nd factors were extracted from the correlation matrix since they could explain totally over 90% variance in all conditions (Table 4-2). Table 4-3 showed the loadings of all energy flow elements in the extracted 1st and 2nd factors with the signs of the loadings determine the direction of the energy flow (flowing in or flowing out). The significant loadings and the signs of the loadings in the 1st/2nd factor were analogous under the conditions in the young adults at the self-selected and fast walking speeds as well as the elderly at the self-selected walking speeds. Thus the energy flow patterns for those three conditions corresponding to the 1st and 2nd factors were summarized as the following two kinds of representative energy flow characteristics. Notably, the significance and sign of the energy flow elements of the elderly at the fast speed were totally opposite to the two representative patterns.

doi:10.6342/NTU201901683

Table 4-1
Correlation coefficient matrix of the eleven energy flow elements.

	Pelvis Distal Flow	Hip Power	Thigh Proximal Flow	Thigh Energy Change Rate	Thigh Distal Flow	Knee Power	Shank Proximal Flow	Shank Energy Change Rate	Shank Distal Flow	Ankle Power	Foot Proximal Flow
Pelvis Distal Flow	-	-0.764	-0.987	-0.699	0.970	-0.837	-0.983	-0.987	0.965	0.039	-0.952
Hip Power	-0.764	-	0.858	0.606	-0.844	0.329	0.710	0.670	-0.732	-0.080	0.719
Thigh Proximal Flow	-0.987	0.858	-	0.708	-0.983	0.748	0.960	0.953	-0.951	-0.051	0.937
Thigh Energy Change Rate	-0.699	0.606	0.708	-	-0.564	0.510	0.580	0.625	-0.533	-0.022	0.526
Thigh Distal Flow	0.970	-0.844	-0.983	-0.564	-	-0.741	-0.969	-0.949	0.971	0.054	-0.957
Knee Power	-0.837	0.329	0.748	0.510	-0.741	-	0.883	0.895	-0.859	0.230	0.866
Shank Proximal Flow	-0.983	0.710	0.960	0.580	-0.969	0.883	-	0.990	-0.993	0.046	0.985
Shank Energy Change Rate	-0.987	0.670	0.953	0.625	-0.949	0.895	0.990	-	-0.967	-0.038	0.953
Shank Distal Flow	0.965	-0.732	-0.951	-0.533	0.971	-0.859	-0.993	-0.967	-	-0.118	-0.997
Ankle Power	0.039*	-0.080*	-0.051*	-0.022*	0.054*	0.230	0.046*	-0.038*	-0.118	-	0.188
Foot Proximal Flow	-0.952	0.719	0.937	0.526	-0.957	0.866	0.985	0.953	-0.997	0.188	-

* Correlation coefficients with poor significance (< 0.1).

Table 4-2
Explained variance of extracted 1st and 2nd factors of the energy flow data in the young adults and the elderly.

	Young Adults		Elderly	
Factor	Self-Selected	Fast	Self-Selected	Fast
1st Factor	57%	60%	50%	62%
2nd Factor	36%	35%	46%	33%
Total	**93%**	**95%**	**96%**	**95%**

doi:10.6342/NTU201901683

Table 4-3
Loadings of energy flow elements in extracted factors for the young adults and elderly during the swing phase at the self-selected and fast walking speeds.

Energy Flow	Young Adults				Elderly			
	Self-Selected		Fast		Self-Selected		Fast	
	1st Factor	2nd Factor	1st Factor	2nd Factor	1st Factor	2nd Factor	1st Factor	2nd Factor
Pelvis Distal Flow	0.79	-0.61	0.80	-0.59	0.70	-0.72	-0.89*	0.45
Hip Power	-0.30	0.91§	-0.38	0.90§	-0.37	0.92§	0.98§	-0.13
Thigh Proximal Flow	-0.70	0.71	-0.74	0.68	-0.59	0.81*	0.94*	-0.34
Thigh Energy Change Rate	-0.27	0.76	-0.04	0.89*	0.05	0.90*	0.80*	0.43
Thigh Distal Flow	0.75	-0.63	0.80	-0.59	0.65	-0.75	-0.88*	0.46
Knee Power	-0.95§	0.13	-0.90*	-0.24	-0.93§	-0.14	0.001	-0.90§
Shank Proximal Flow	-0.87*	0.49	-0.90*	0.44	-0.81*	0.59	0.78	-0.62
Shank Energy Change Rate	-0.87*	0.48	-0.85*	0.51	-0.73	0.67	0.89*	-0.45
Shank Distal Flow	0.86*	-0.48	0.93*	-0.37	0.86*	-0.50	-0.65	0.76
Foot Proximal Flow	-0.87*	0.47	-0.93§	0.33	-0.87*	0.46	0.62	-0.77

* Significant absolute loading (> 0.8); § Highest loading in each column.

doi:10.6342/NTU201901683

4.3 Swing energy flow characteristics shown in simplified energy flow diagram

The first representative energy flow characteristics could be patterned in terms of the 1st factor, which was with highest loading at the knee power, with most significant loadings below the knee joint, and insignificant hip power and thigh energy change rate (Table 4-3). This characteristic accordingly showed a knee-dominated pattern. It was noted that the signs of the energy flow elements in this pattern perfectly agreed with the signs of the energy flow profiles during the late stage of the swing phase as shown in Figure 4-1. Thus, the knee-dominated pattern represents the energy flow characteristic of swing deceleration. It could be illustrated as an upward energy transfer since there was a substantial amount of energy flowing from the foot all the way up to the pelvis and the segmental energy change rates decreased together with the knee power absorption. The second energy flow characteristic could be found in the 2nd factor with highest loading at the hip energy flow and most significant loadings above the knee joint. Since the signs of the energy flow elements of this hip-dominated pattern agreed with the signs of the energy flow profiles during the early stage of the swing, this pattern shows the energy flow characteristic of swing acceleration. It can also be depicted as a downward energy transfer for the segmental

doi:10.6342/NTU201901683

energy change rates increased together with the hip power generation (Figure 4-2a-2c). Following the same process to reveal the energy flow pattern of the elderly during the fast walking, different patterns were observed that the 1st factor oppositely corresponds to swing acceleration with the signs of the loadings agreed with those in the 2nd factor of the representative energy flow, and that the 2nd factor of the elderly during the fast walking corresponds to swing deceleration. In addition, the high-loading energy flow elements in this condition were especially above the knee during the swing acceleration, and there was a centered pattern exclusively at the knee power during the swing deceleration (Figure 4-2d).

Condition	Swing Acceleration	Swing Deceleration
(a) Young adults, Self-selected	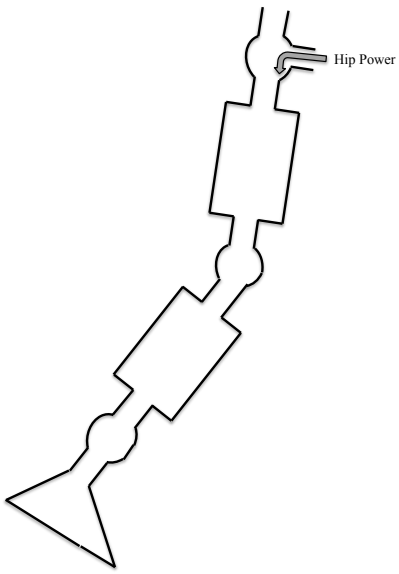	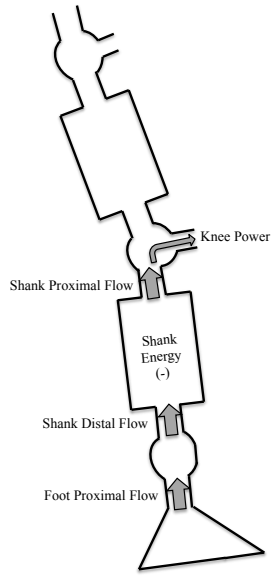

doi:10.6342/NTU201901683

(b) Young adults, Fast	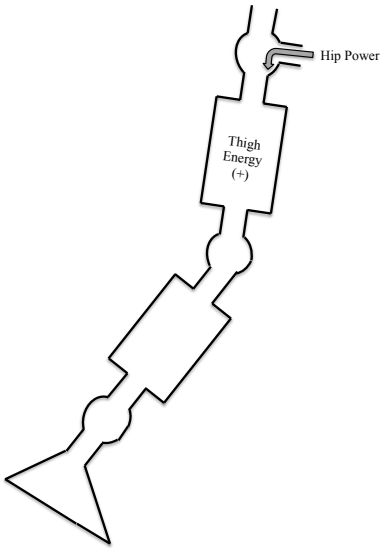	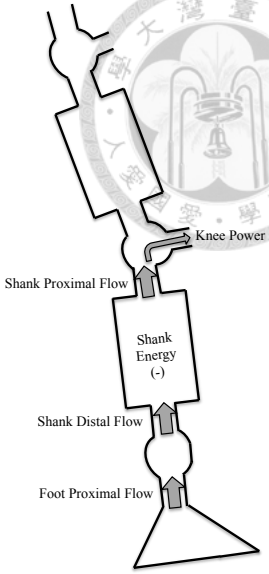
(c) Elderly, Self-selected	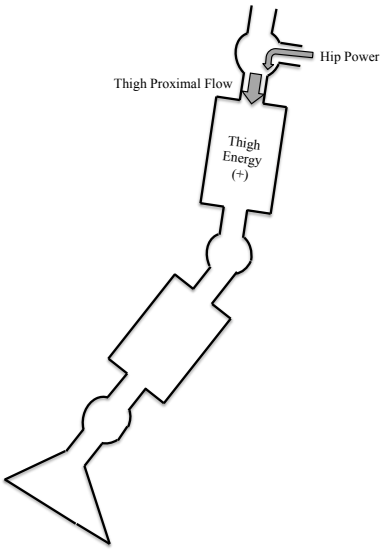	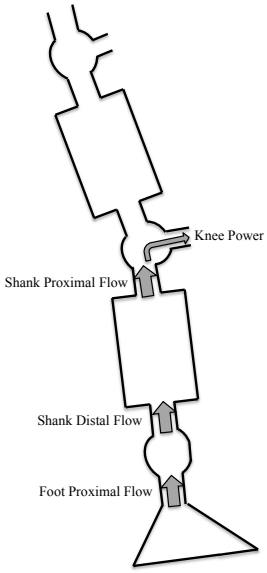
(d) Elderly, Fast	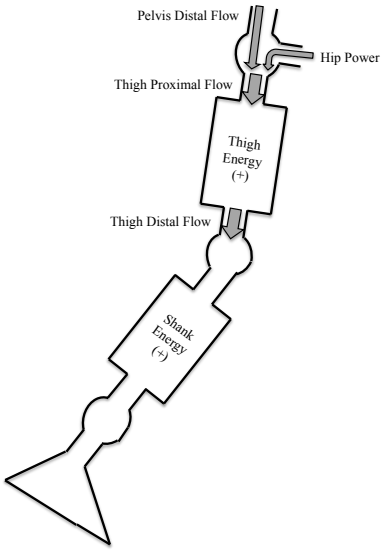	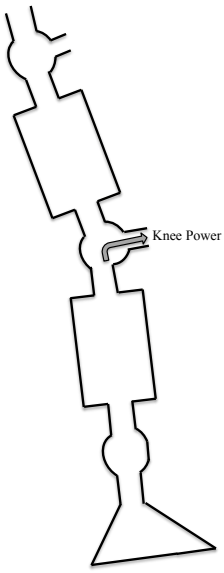

doi:10.6342/NTU201901683

Figure 4-2 Energy flow patterns corresponding to the swing acceleration and swing deceleration in the young adults and the elderly at the self-selected and fast walking speeds.

doi:10.6342/NTU201901683

4.4 Discussion

This study demonstrated a systematic approach to extract the energy flow characteristics of the swing leg in the young adults and elderly. The major findings were: 1) the energy flows of the swing leg showed different patterns between the early swing and the late swing with negligible ankle power; 2) the young adults showed similar energy flow characteristics of the swing leg for both fast and self-selected walking speeds, while the elderly showed an especially opposite energy flow pattern at the fast walking speed; and 3) the hip power and the knee power mainly correspond to the swing acceleration and deceleration, respectively. Our work demonstrated a valuable analytic scheme to explore the changes of the gait characteristics and potentially the mechanisms of the tripping risk in elderly.

Energy flow analysis is a powerful tool to observe the energy transfer through the segment compared to the traditional joint angle or joint moment analysis. In this study, the representative energy flow pattern of the entire lower extremity clearly visualize the difference of the energy transfer between the early phase and late phase of the swing leg. During the early swing phase, the energy source to propel the lower extremity could be composited of the negative pelvis distal flow (i.e. energy flowing

doi:10.6342/NTU201901683

out of the distal pelvis) and the positive hip power (i.e. energy generation from the hip), collectively transfer into the thigh and then the shank, with the trivial knee power (Figure 4-1a). This downward energy was partially contributed by the thigh and shank with positive thigh energy change rate and shank energy change rate (Figure 4-1e), and the shank distal flow eventually become the energy source of the foot due to the insignificant role of the ankle power (Figure 4-1i). During the late swing phase, which is also known as the deceleration phase of the swing leg, substantial amount of the stored energy in the whole swing leg required to be released by means of the negative thigh, shank, and foot energy change rate and the released energy was primarily absorbed by the knee joint, i.e. the negative knee power. Thus the energy flow analysis could be used to reveal the transfer of the mechanical energy across multiple segments and joints of a swing leg.

The energy flow model showed the merit to illustrate the changes of the different sources of energy throughout the lower extremity based on the energy-time plot. Nevertheless, it could only be noted that the elderly at the fast walking speed especially showed the great energy fluctuation and great individual variations upon the comparisons among the different conditions (e.g. the young adults and elderly at the

doi:10.6342/NTU201901683

self-selected or the fast walking speed) (Figure 4-1). In addition, there's no clear definition of the time event in the swing phase of the gait for the dedicated comparisons among the conditions. Although researchers/clinicians usually acknowledge that the swing phase consists of the acceleration and deceleration stage, unlike the well-defined time events such as heel strike, heel off, and toe off during the stand phase, the definitions for the initial swing, mid-swing, and terminal swing stage are vague given that the swing limb is off the ground. The high-dimensional and temporal-dependent characteristics of the energy flow elements in different conditions still need a systematic method to be easily compared and comprehended.

The energy flow model utilized in previous studies mostly focused on analyzing an instant gait event [50, 51]. The current study applied the factor analysis to reduce the high-dimensional dataset and showed that the hip power and knee power typically correspond to the acceleration and deceleration phase of the leg swing respectively. As a representative pattern in the young subject at the self-selected walking speed, the 1st factor highly covaried with energy flow elements especially below the knee (i.e., the knee power, the shank proximal flow, the shank energy change rate, the shank distal flow, and the foot proximal flow) with mostly being negative which means the energy

doi:10.6342/NTU201901683

was expelled from the segment/joint (Table 4-3). Moreover, this flow pattern was dominated by the knee power absorption among those high-loading parameters. As shown in Figure 4-2a, the knee-dominated flow pattern could be visualized as an upward energy transfer, i.e. the energy flows from distal to proximal for absorbing the segmental energy. Accordingly, the 1st factor could be the governing factor for swing deceleration during the late swing. On the other hand, the 2nd factor mainly attributed to the energy flow elements above the knee with positive values which means the energy was gained in the segment/joint. This pattern was dominated by hip power generation with highest loadings. Thus the 2nd factor was a hip-dominated flow pattern with a downward energy transfer from proximal to distal for storing the segmental energy and corresponds to the leg acceleration during the early swing. The current results evidenced the previous conception that the hip power and knee power play roles during the early and late swing phases [34]. The current study further showed that the 1st factor explained more variance than the 2nd factor (Table 4-2), which could imply that people put more efforts on the deceleration than acceleration.

The identified energy flow patterns based on the factor analysis also help to reveal the difference in the control mechanism of the lower extremity between the

doi:10.6342/NTU201901683

young adults and elderly. In young adults at the self-selected and fast walking speeds, the energy flow characteristic was functionally analogous, that is, the knee power dominated the 1st factor to decelerate the swing leg, while the hip power dominated the 2nd factor for leg acceleration. The elderly showed similar characteristics to the young adults at self-selected speed. But their pattern changed fundamentally at the fast walking speed such that the 1st factor oppositely became the governing factor for the leg acceleration since the high-loading energy flow elements were mostly positive and above the knee, and the 2nd factor became the one corresponded to the swing deceleration, i.e. the high-loading energy flow elements were mostly negative and below the knee. Compared to the corresponding energy flow patterns of the young adults, the 1st factor of the elderly during the fast walking showed the overwhelming highest loading at the hip power, and the 2nd factor showed a centered high loading pattern exclusively at the knee power (Table 4-3). In addition, the 1st factor for swing acceleration in elderly at the fast walking explained even more variance than the 1st factor for swing deceleration in other conditions (Table 4-2). In other words, during the fast walking, the elderly especially put more efforts on the acceleration than the deceleration. Judge et al. reported that the hip flexor power in elderly would increase

doi:10.6342/NTU201901683

not only for assisting swing leg advancement but also for compensating the decreased ankle plantarflexor power [36]. De-Vita and Hortobagyi also found that the hip extensor moment and power would increase together with a reduction of ankle and knee power in elderly at the fast walking speed [26]. The enhanced role of the hip to drive the swing could increase the propelling speed of the leg at the cost of augmenting the sway of the center of mass around the lumbar area. Moreover, the great reliance on the knee to decelerate the swing leg and the reduced efforts on the deceleration may increase the difficulty to precisely place the foot. Thus those compensative strategies used by the elderly could be the reasons leading to the tripping or even fall when they perform a challenged walking such as crossing the street, chasing the bus, or doing a brisk walk exercise.

Several study limitations should be addressed. First, only the energy characteristics during the swing phase were discussed. The swing phase is the focus of this study because the unsuccessful advancement of the leg could be critical issues on tripping in the elderly. Our study was the first to systematically reveal to distinguishable difference of the energy flow characteristics of the swing leg in elderly. Second, the energy flow analysis in this study focused on the energy changes of the

doi:10.6342/NTU201901683

segments rather than the energy magnitudes. The magnitudes of the energy vary among subjects, but the pattern of the energy changes across the segments would be analogous and could be appropriate for revealing the control strategy of human movements. Finally, the mechanical energy discussed in this study was to highlight the personal ability to drive the limb against the surrounding challenges. Future study was warranted to incorporate with the electromyography or the cardiopulmonary function measures to facilitate the understanding of the comprehensive energy transfer both mechanically and biologically.

In summary, the young adults demonstrated similar energy flow characteristics of the swing leg at both the fast and the self-selective walking speeds, in which they put more efforts on the swing deceleration than on the swing acceleration. Nevertheless, the elderly showed a distinct energy flow pattern at the fast walking that they put significantly great hip and thigh efforts on the swing acceleration but exclusively rely on the knee function to decelerate the swing leg, which might lead to an unstable gait.

doi:10.6342/NTU201901683

Chapter 5
Conclusions

We had developed an energy flow model for intuitively identifying movement strategy by observing the energy flow characteristics in terms of flow pattern and energy distribution. New symbolic convention in the developed energy flow diagram facilitates the conceptualization of mechanical energy transfer between body segments as water flowing through a system of pipes, storage tanks, and pumps. Such comparison allows readers use their understanding of a more familiar system and fluid flow to intuit energy transfer within the body. The beauty of the proposed model is to graphically interpret the specific movement strategy in a systematic view rather than focusing on a single joint/segment. Key terms of the energy flows within the model such as joint power or segmental energy change rate are already widely used in clinical research and therefore previous knowledge can directly fit into the proposed model. Another feature of this model is that it is easy to implement from various commercial motion analysis software.

Our results have demonstrated the proposed energy flow analysis can lay a foundation of the energy utilization in human gait and from where the role of joint

doi:10.6342/NTU201901683

powers can be further clarified. This research also explicitly revealed the energy change processes occurred during the leg advancement, and the factor analysis to be able to compare the energy flow characteristics in different subject groups. We expect that many unexplored movement strategies can be found under a systematic view constructed by the proposed energy flow model in the future. Not only to human gait, the energy flow diagram with the symbolic convention can also be employed to track the energy source(s) of the movements performed by elite athletes in order to design better training programs. Similarly, this energy flow diagram can be a useful tool that assists research across disciplines in studying clinical intervention of rehabilitation and innovations in exoskeletal robotics.

Future works of this research will be:

1. Corelate the physiological energy with the mechanical energy by taking consideration of muscle co-contraction.
2. Reduce the high-dimensional dataset for factor analysis.
3. Automatic identification of energy flow characteristics in real-time.

doi:10.6342/NTU201901683

References

[1] Winter, D. A., & Robertson, D. G. E. (1978). Joit torque and energy patterns in normal gait. Biological cybernetics, 29(3), 137-142.

[2] Guo, L. Y., Su, F. C., Wu, H. W., & An, K. N. (2003). Mechanical energy and power flow of the upper extremity in manual wheelchair propulsion. Clinical Biomechanics, 18(2), 106-114.

[3] Guo, L. Y., Su, F. C., & An, K. N. (2006). Effect of handrim diameter on manual wheelchair propulsion: mechanical energy and power flow analysis. Clinical biomechanics, 21(2), 107-115.

[4] Huang, Y. C., Guo, L. Y., Tsai, C. Y., & Su, F. C. (2013). Mechanical energy and power flow analysis of wheelchair use with different camber settings. Computer methods in biomechanics and biomedical engineering, 16(4), 403-412.

[5] Kerrigan, D. C., Todd, M. K., Della Croce, U., Lipsitz, L. A., & Collins, J. J. (1998). Biomechanical gait alterations independent of speed in the healthy elderly: evidence for specific limiting impairments. Archives of Physical Medicine and Rehabilitation, 79(3), 317-322.

[6] Winter, D. A., Patla, A. E., Frank, J. S., & Walt, S. E. (1990). Biomechanical walking pattern changes in the fit and healthy elderly. Physical Therapy, 70(6), 340-347.

doi:10.6342/NTU201901683

[7] Winter, D. A. (1983). Energy generation and absorption at the ankle and knee during fast, natural, and slow cadences. Clinical Orthopaedics and Related Research, 175, 147-154.

[8] Kepple, T. M., Siegel, K. L., & Stanhope, S. J. (1997). Relative contributions of the lower extremity joint moments to forward progression and support during gait. Gait & Posture, 6(1), 1-8.

[9] Garcia, M., Chatterjee, A., Ruina, A., & Coleman, M. (1998). The simplest walking model: stability, complexity, and scaling. Journal of Biomechanical Engineering, 120(2), 281-288.

[10] McGeer, T. (1990). Passive Dynamic Walking. The International Journal of Robotics Research, 9(2), 62-82.

[11] Wisse, M. (2005). Three additions to passive dynamic walking: actuation, an upper body, and 3D stability. International Journal of Humanoid Robotics, 2(04), 459-478.

[12] Alexander, R. M. (2005). Walking made simple. Science, 308(5718), 58-59.

[13] Perry, J. (1974). Kinesiology of lower extremity bracing. Clinical Orthopaedics and Related Research, 102, 18-31.

[14] Simon, S. R., Mann, R. A., Hagy, J. L., & Larsen, L. J. (1978). Role of the posterior calf muscles in normal gait. The Journal of Bone and Joint Surgery. American volume, 60(4), 465-472.

[15] Sutherland, D. H., Cooper, L., & Daniel, D. (1980). The role of the ankle plantar flexors in normal walking. The Journal of Bone and Joint Surgery. American volume, 62(3), 354-363.

doi:10.6342/NTU201901683

[16] Bajd, T., Kralj, A., Karcnik, T., Savrin, R., Benko, H., & Obreza, P. (1997). Influence of electrically stimulated ankle plantar flexors on the swinging leg. Artificial Organs, 21(3), 176-179.

[17] Meinders, M., Gitter, A., & Czerniecki, J. M. (1998). The role of ankle plantar flexor muscle work during walking. Scandinavian Journal of Rehabilitation Medicine, 30(1), 39-46.

[18] Lipfert, S. W., Günther, M., Renjewski, D., & Seyfarth, A. (2014). Impulsive ankle push-off powers leg swing in human walking. Journal of Experimental Biology, 217(8), 1218-1228.

[19] Renjewski, D., & Seyfarth, A. (2012). Robots in human biomechanics--a study on ankle push-off in walking. Bioinspiration & Biomimetics, 7(3), 036005.

[20] Neptune, R. R., Kautz, S. A., & Zajac, F. E. (2001). Contributions of the individual ankle plantar flexors to support, forward progression and swing initiation during walking. Journal of Biomechanics, 34(11), 1387-1398.

[21] Liu, M. Q., Anderson, F. C., Schwartz, M. H., & Delp, S. L. (2008). Muscle contributions to support and progression over a range of walking speeds. Journal of Biomechanics, 41(15), 3243-3252.

[22] Caputo, J. M., & Collins, S. H. (2014). Prosthetic ankle push-off work reduces metabolic rate but not collision work in non-amputee walking. Scientific Reports, 4, 7213.

[23] Blanke, D. J., & Hageman, P. A. (1989). Comparison of gait of young men and elderly men. Physical Therapy, 69(2), 144-148.

doi:10.6342/NTU201901683

[24] Chung, M. J., & Wang, M. J. J. (2010). The change of gait parameters during walking at different percentage of preferred walking speed for healthy adults aged 20–60 years. Gait & posture, 31(1), 131-135.

[25] Boyer, K. A., Andriacchi, T. P., & Beaupre, G. S. (2012). The role of physical activity in changes in walking mechanics with age. Gait & posture, 36(1), 149-153.

[26] DeVita, P., & Hortobagyi, T. (2000). Age causes a redistribution of joint torques and powers during gait. Journal of applied physiology, 88(5), 1804-1811.

[27] Graf, A., Judge, J. O., Õunpuu, S., & Thelen, D. G. (2005). The effect of walking speed on lower-extremity joint powers among elderly adults who exhibit low physical performance. Archives of physical medicine and rehabilitation, 86(11), 2177-2183.

[28] Riley, P. O., Della Croce, U., & Kerrigan, D. C. (2001). Effect of age on lower extremity joint moment contributions to gait speed. Gait & posture, 14(3), 264-270.

[29] Boyer, K. A., Johnson, R. T., Banks, J. J., Jewell, C., & Hafer, J. F. (2017). Systematic review and meta-analysis of gait mechanics in young and older adults. Experimental gerontology, 95, 63-70.

[30] McGibbon, C. A. (2003). Toward a better understanding of gait changes with age and disablement: neuromuscular adaptation. Exercise and sport sciences reviews,

doi:10.6342/NTU201901683

31(2), 102-108.

[31] Begg, R., Best, R., Dell'Oro, L., & Taylor, S. (2007). Minimum foot clearance during walking: strategies for the minimisation of trip-related falls. Gait & posture, 25(2), 191-198.

[32] Lai, D. T., Taylor, S. B., & Begg, R. K. (2012). Prediction of foot clearance parameters as a precursor to forecasting the risk of tripping and falling. Human movement science, 31(2), 271-283.

[33] Launay, C., De Decker, L., Annweiler, C., Kabeshova, A., Fantino, B., & Beauchet, O. (2013). Association of depressive symptoms with recurrent falls: a cross-sectional elderly population based study and a systematic review. The journal of nutrition, health & aging, 17(2), 152-157.

[34] Eng, J. J., & Winter, D. A. (1995). Kinetic analysis of the lower limbs during walking: what information can be gained from a three-dimensional model?. Journal of biomechanics, 28(6), 753-758.

[35] McGibbon, C. A., Puniello, M. S., & Krebs, D. E. (2001). Mechanical energy transfer during gait in relation to strength impairment and pathology in elderly women. Clinical Biomechanics, 16(4), 324-333.

doi:10.6342/NTU201901683

[36] JudgeRoy, J. O., Davis III, B., & Õunpuu, S. (1996). Step length reductions in advanced age: the role of ankle and hip kinetics. The Journals of Gerontology Series A: Biological Sciences and Medical Sciences, 51(6), M303-M312.

[37] Siegel, K. L., Kepple, T. M., & Stanhope, S. J. (2004). Joint moment control of mechanical energy flow during normal gait. Gait & posture, 19(1), 69-75.

[38] McGibbon, C. A., Krebs, D. E., & Puniello, M. S. (2001). Mechanical energy analysis identifies compensatory strategies in disabled elders' gait. Journal of biomechanics, 34(4), 481-490.

[39] De Leva, P. (1996). Adjustments to Zatsiorsky-Seluyanov's segment inertia parameters. Journal of Biomechanics, 29(9), 1223-1230.

[40] Bell, A. L., Brand, R. A., & Pedersen, D. R. (1987). Prediction of hip joint center location from external landmarks. Journal of Biomechanics, 20(9), 913.

[41] Siegel, K. L., Kepple, T. M., & Caldwell, G. E. (1996). Improved agreement of foot segmental power and rate of energy change during gait: inclusion of distal power terms and use of three-dimensional models. Journal of Biomechanics, 29(6), 823-827.

[42] Takahashi, K. Z., Kepple, T. M., & Stanhope, S. J. (2012). A unified deformable (UD) segment model for quantifying total power of anatomical and prosthetic below-

doi:10.6342/NTU201901683

knee structures during stance in gait. Journal of Biomechanics, 45(15), 2662-2667.

[43] Takahashi, K. Z., & Stanhope, S. J. (2013). Mechanical energy profiles of the combined ankle–foot system in normal gait: insights for prosthetic designs. Gait & Posture, 38(4), 818-823.

[44] McGinley, J., Goldie, P., Greenwood, K., & Olney, S. (2003). Accuracy and reliability of observational gait analysis data: Jugments of push-off in gait after stroke. Physical Therapy, 83(2), 146-160.

[45] Desloovere, K., Molenaers, G., Van Gestel, L., Huenaerts, C., Van Campenhout, A., Callewaert, B., et al. (2006). How can push-off be preserved during use of an ankle foot orthosis in children with hemiplegia? A prospective controlled study. Gait & Posture, 24(2), 142-151.

[46] Morgenroth, D. C., Segal, A. D., Zelik, K. E., Czerniecki, J. M., Klute, G. K., Adamczyk, P. G., et al. (2011). The effect of prosthetic foot push-off on mechanical loading associated with knee osteoarthritis in lower extremity amputees. Gait & Posture, 34(4), 502-507.

[47] Gordon, D., Robertson, E., & Winter, D. A. (1980). Mechanical energy generation, absorption and transfer amongst segments during walking. Journal of

doi:10.6342/NTU201901683

biomechanics, 13(10), 845-854.

[48] Zelik, K. E., Takahashi, K. Z., & Sawicki, G. S. (2015). Six degree-of-freedom analysis of hip, knee, ankle and foot provides updated understanding of biomechanical work during human walking. Journal of Experimental Biology, 218(6), 876-886.

[49] Buczek, F. L., Kepple, T. M., Siegel, K. L., & Stanhope, S. J. (1994). Translational and rotational joint power terms in a six degree-of-freedom model of the normal ankle complex. Journal of Biomechanics, 27(12), 1447-1457.

[50] Simonsen, E. B. (2014). Contributions to the understanding of gait control. University of Copenhagen.

[51] McGibbon, C. A., & Krebs, D. E. (1999). Effects of age and functional limitation on leg joint power and work during stance phase of gait. Journal of rehabilitation research and development, 36(3), 173-182.

doi:10.6342/NTU201901683

Appendix I

Informed Consent

國立台灣大學醫學院附設醫院
臨床試驗/研究受試者說明及同意書

您被邀請參與此臨床試驗/研究，這份表格提供您本試驗/研究之相關資訊，本試驗/研究已取得研究倫理委員會審查通過，研究主持人或其授權人員將會為您說明研究內容並回答您的任何疑問，請您經過慎重考慮後方予簽名。您須簽署同意書後才能參與本試驗/研究。

研究計畫名稱： 中文：以老年人為例探討步態機械能流動特徵與動作策略 英文：Mechanical Energy Flow Characteristics and Movement Strategy in Human Gait: Application to the Elders
執行單位：　台灣大學醫學工程學研究所　委託單位/藥廠：　無 主要主持人：　章良渭　職稱：副教授　電話：(02)33663298 ※二十四小時緊急聯絡人：　陳鴻彬　電話：0958939562
受試者姓名： 性別：　出生日期： 病歷號碼： 通訊地址： 聯絡電話： 法定代理人、輔助人或有同意權人之姓名： 與受試者關係：

doi:10.6342/NTU201901683

性別：　　出生日期：

身分證字號：

通訊地址：

聯絡電話：

一、藥品、醫療技術、醫療器材全球上市現況簡介：

本研究不涉及藥品、醫療技術、醫療器材。

二、試驗目的：

藉由分析健康老年人之步行特徵，提供未來銀髮族行動輔具設計之參考。健康青壯年受試者之步態屬對照用途。

三、試驗之主要納入與排除條件：

負責本研究的人員會幫您做評估，並與您討論參加本研究所必需的條件。您必須在進入研究前簽署本受試者說明及同意書。

納入條件：

您必須符合以下所有條件方能參加本研究：

1. 能接受並執行試驗指令
2. 四肢功能健全

排除條件：

若有下列任何情況者，不能參加本研究：

1. 四肢功能受損
2. 需他人攙扶或使用拐杖等器具方可行走

四、試驗方法及相關檢驗：

本研究將透過三維動作分析系統、測力板、肌電圖儀與耗氧量分析儀紀錄您步行時之動作、力學與能量參數。首先請您先填寫基本資料，接著將為您丈量身材並進行臨床評估，專業臨床人員將評估您的關節活動度與肌力。進行量測前，我們將於您身上貼標記與肌電圖貼片，再由三維動作分析儀、測力板與肌電圖儀取得您步行時之動作與力學資料，由耗氧量分析儀取得您步行時之能量資料。三維動作測試時，首先您將以最舒服之速率，以同方向直線走過約六公尺步道共走三趟。之後會再請您以較最舒服之速率稍慢與稍快之速率，重複上述動作測試實驗。耗氧量測試時，將請您配戴量測面罩，以最舒服之速率，依指定路徑走過約三十公尺步道共走三趟，每趟行走後您可以休息十~二十分鐘；休息後再請您以較最舒服之速率稍慢與稍快之速率，依指

doi:10.6342/NTU201901683

定路徑再各走三趟，重複上述耗氧量實驗。試驗花費總時間約為兩小時。

五、剩餘檢體處理情形：

本研究無採集檢體。

六、可能產生之副作用、發生率及處理方法：

1. 測試過程會有至少兩位臨床人員隨時在旁注意您的安全，避免跌倒。
2. 研究過程中所須蒐集之步態動作資料乃由非侵入性的量測方式取得，也沒有對人體會造成傷害的能量進入體內，所有儀器皆為廣為使用之市售研究設備，絕不會造成傷害。

七、其他替代療法及說明：

本研究不涉及臨床醫療處置。

八、試驗預期效益：

本研究探討之健康老年人步行特徵，可能提供未來銀髮族行動輔具設計之重要參考。

九、試驗進行中受試者之禁忌、限制與應配合之事項：

每次試驗進行時請配合研究人員之指示步行指定路線。

十、機密性：

臺大醫院將依法把任何可辨識您的身分之記錄與您的個人隱私資料視為機密來處理，不會公開。如果發表試驗結果，您的身分仍將保密。您亦瞭解若簽署同意書即同意您的原始醫療紀錄可直接受監測者、稽核者、研究倫理委員會及主管機關檢閱，以確保臨床試驗過程與數據符合相關法律及法規要求；上述人員並承諾絕不違反您的身分之機密性。

十一、損害補償與保險：

（一）如依本研究所訂臨床試驗計畫，因而發生不良反應或損害，本醫院願意提供專業醫療照顧及醫療諮詢。您不必負擔治療不良反應或傷害之必要醫療費用。

（二）您不會因為簽署本同意書，而喪失在法律上的任何權利。

doi:10.6342/NTU201901683

十二、受試者權利：

（一）試驗過程中，與您的健康或是疾病有關，可能影響您繼續接受臨床試驗意願的任何重大發現，都將即時提供給您。

（二）新台幣五百元之車馬費將在每次參與試驗後發給您。

（三）本試驗已經過本院研究倫理委員會審查，並已獲得核准。本院研究倫理委員會委員由醫事專業人員、法律專家、社會工作人員及其他社會公正人士所組成，每月開會一次，審查內容包含試驗之利益及風險評估、受試者照護及隱私保護等。如果您在試驗過程中對試驗工作性質產生疑問，對身為患者之權利有意見或懷疑因參與研究而受害時，可與本院之研究倫理委員會聯絡請求諮詢，其電話號碼為：（02)2312-3456 轉 63155 。

（四)為進行試驗工作，您必須接受 章良渭 副教授的照顧。如果您現在或於試驗期間有任何問題或狀況，請不必客氣，可與在台灣大學醫學工程學研究所的章良渭 副教授聯絡(24 小時聯繫電話：0958939562)。

本同意書一式 2 份，醫師已將同意書副本交給您，並已完整說明本研究之性質與目的。章良渭 副教授已回答您有關研究的問題。

十三、試驗之退出與中止：

您可自由決定是否參加本試驗；試驗過程中也可隨時撤銷同意，退出試驗，不需任何理由，且不會引起任何不愉快或影響日後醫師對您的醫療照顧。試驗主持人亦可能於必要時中止該試驗之進行。

十四、簽名

（一）主要主持人、協同主持人已詳細解釋有關本研究計畫中上述研究方法的性質與目的，及可能產生的危險與利益。

主要主持人/協同主持人簽名：

日期：□□□□年□□月□□日

（二）受試者已詳細瞭解上述研究方法及其所可能產生的危險與利益，有關本試驗計畫的疑問，業經計畫主持人詳細予以解釋。本人同意接受為臨床試驗計畫的自願受試者。

受試者簽名：

日期：□□□□年□□月□□日

doi:10.6342/NTU201901683

Appendix II

Mean energetic data of lower limb

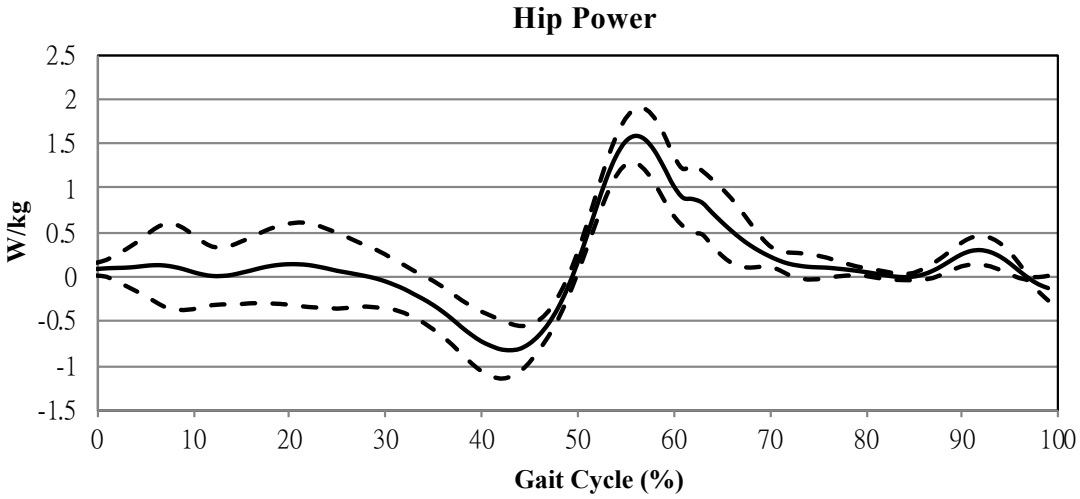

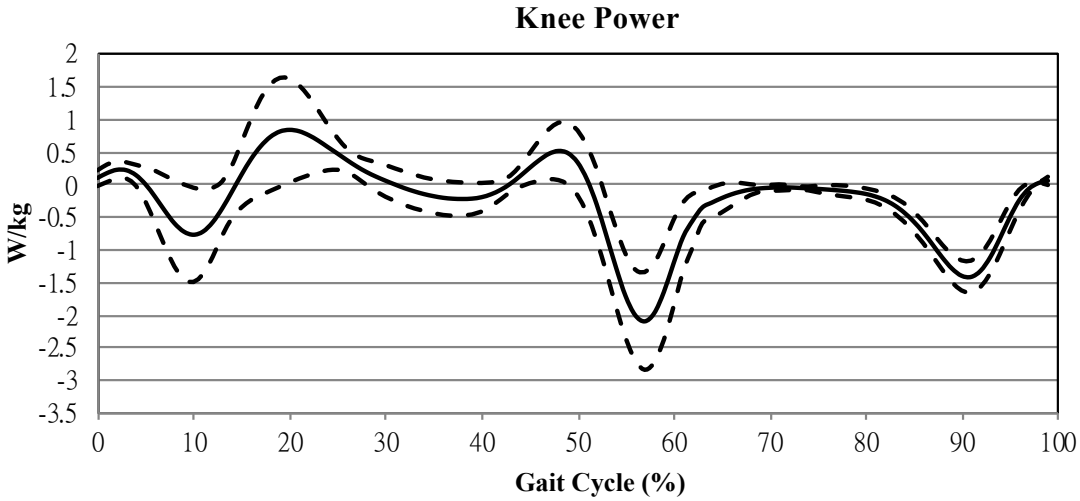

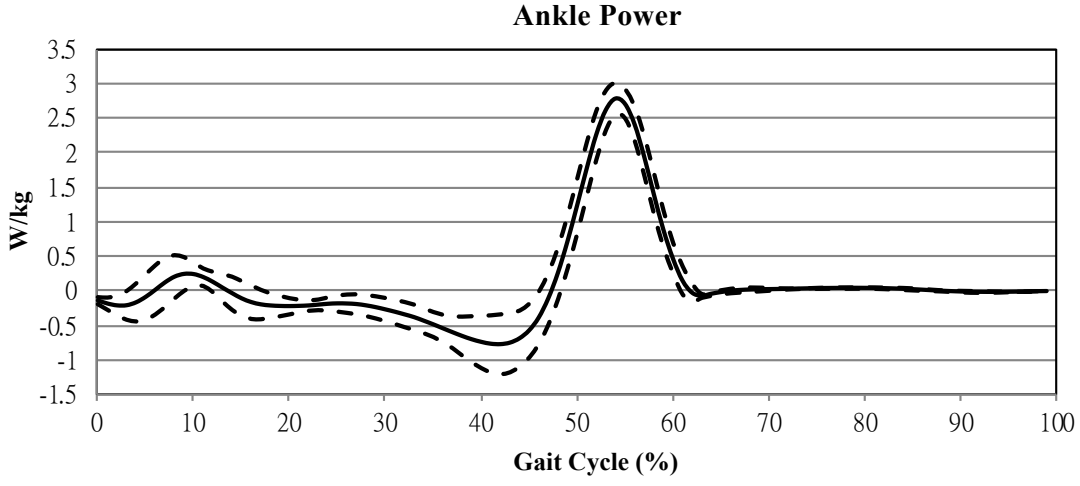

doi:10.6342/NTU201901683

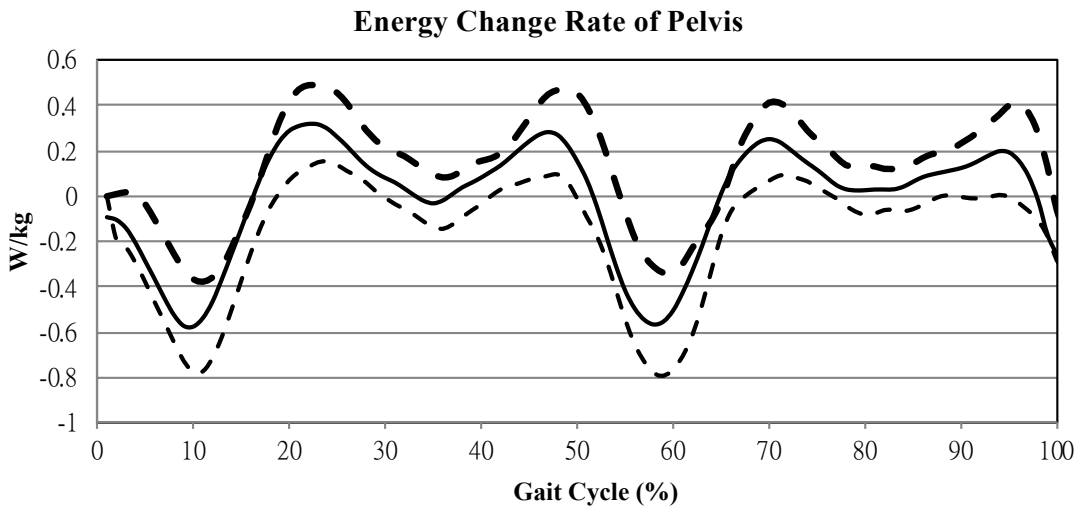

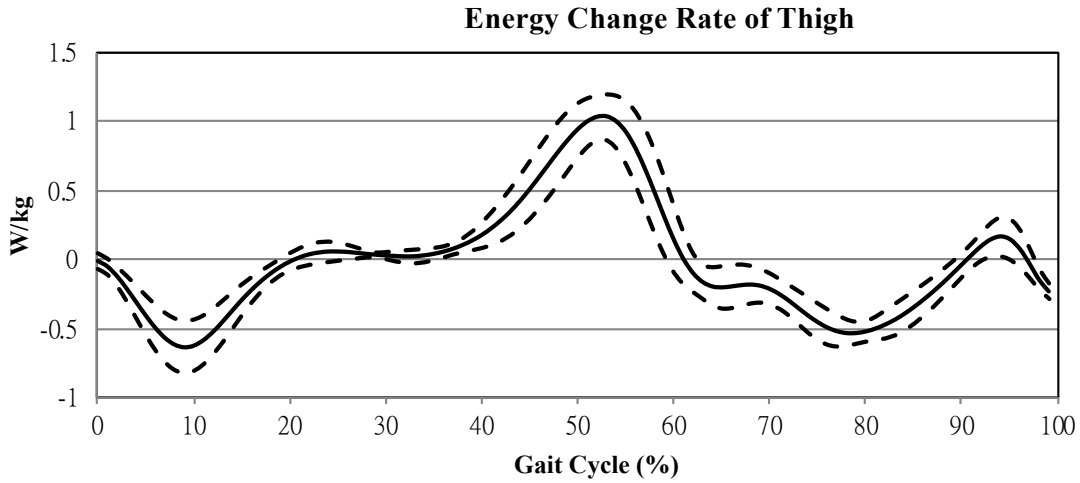

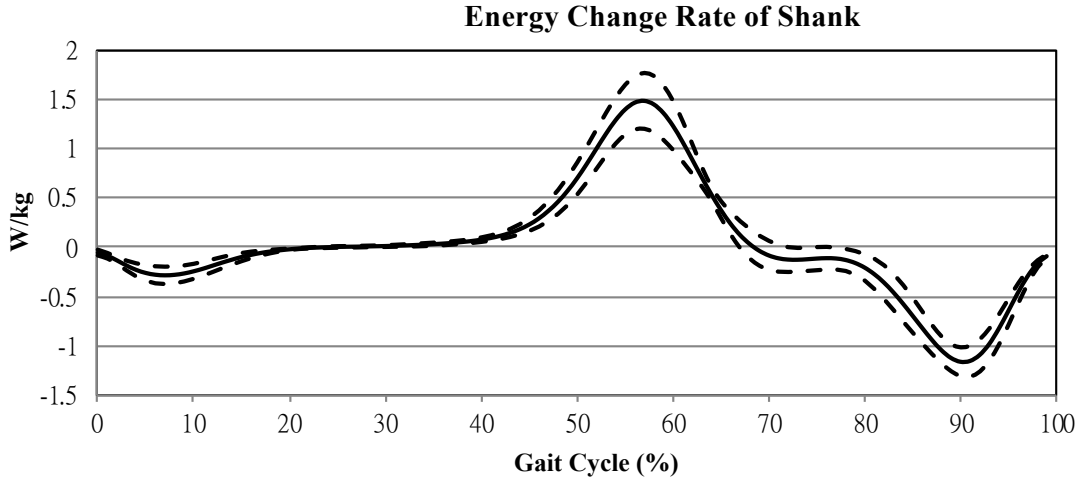

doi:10.6342/NTU201901683

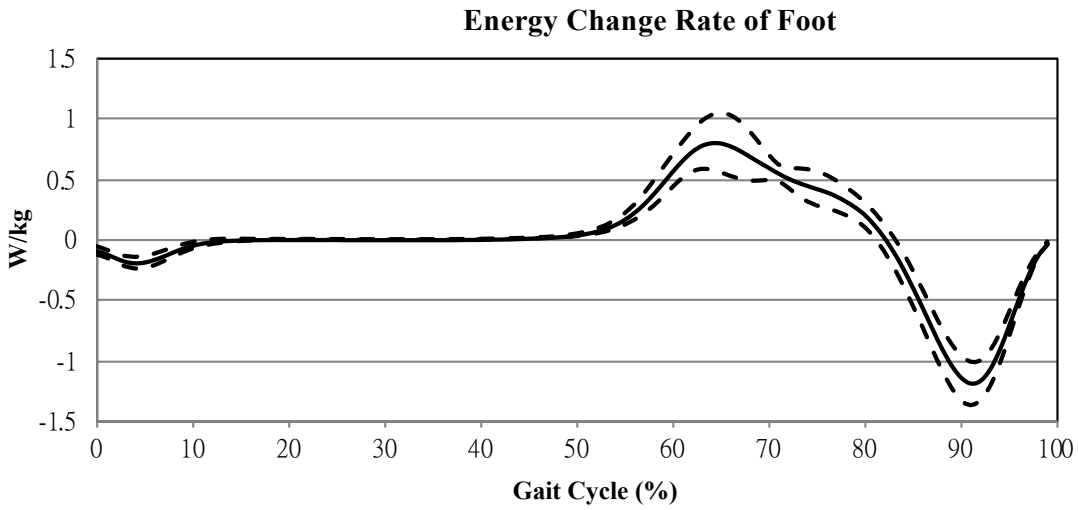

doi:10.6342/NTU201901683